

2 Flood risk reduction and flow buffering as ecosystem  
3 services: I. Theory on flow persistence, flashiness and base  
4 flow

5 Meine van Noordwijk<sup>1,2</sup>, Lisa Tanika<sup>1</sup>, Betha Lusiana<sup>1</sup>

6 [1]{World Agroforestry Centre (ICRAF), SE Asia program, Bogor, Indonesia}

7 [2]{Wageningen University and Research, Plant Production Systems, Wageningen, the Netherlands}

8 Correspondence to: Meine van Noordwijk ([m.vannoordwijk@cgiar.org](mailto:m.vannoordwijk@cgiar.org))

9 **Abstract**

10 Flood damage reflects insufficient adaptation of human presence and activity to location and  
11 variability of river flow in a given climate. Flood risk increases when landscapes degrade,  
12 counteracted or aggravated by engineering solutions. Efforts to maintain and restore  
13 buffering as ecosystem function may help adaptation to climate change, but require  
14 quantification of effectiveness in their specific social-ecological context. However, the  
15 specific role of forests, trees, soil and drainage pathways in flow buffering, given geology,  
16 land form and climate, remains controversial. Complementing the scarce heavily  
17 instrumented catchments with reliable long-term data, especially in the tropics, there is a  
18 need for metrics for data-sparse conditions. We present and discuss a flow persistence  
19 metric that relates transmission to river flow of peak rainfall events, to the base flow  
20 component of the water balance. The dimensionless flow persistence parameter  $F_p$  is  
21 defined in a recursive flow model and can be estimated from limited time series of observed  
22 daily flow, without requiring knowledge of spatially distributed rainfall upstream. The  $F_p$   
23 metric (or its change over time from what appears to be the local norm) matches local  
24 knowledge concepts. Inter-annual variation in the  $F_p$  metric in sample watersheds correlates  
25 with variation in the 'flashiness index' used in existing watershed health monitoring  
26 programs, but the relationship between these metrics varies with context. Inter-annual  
27 variation in  $F_p$  also correlates with common base-flow indicators, but again in a way that  
28 varies between watersheds. Further exploration of the responsiveness of  $F_p$  in watersheds  
29 with different characteristics to the interaction of land cover and the specific realization of  
30 space-time patterns of rainfall in a limited observation period is needed to evaluate  
31 interpretation of  $F_p$  as indicator of anthropogenic changes in watershed condition.

32 **1 Introduction**

33 Floods can be the direct result of reservoir dams, log jams or protective dykes breaking, with water  
34 derived from unexpected heavy rainfall, rapid snow melt, tsunamis or coastal storm surges. We  
35 focus here on floods that are associated, at least in the public eye, with watershed degradation.  
36 Degradation of watersheds and its consequences for river flow regime and flooding intensity and  
37 frequency are a widespread concern (Brauman et al., 2007; Bishop and Pagiola, 2012; Winsemius et  
38 al., 2013). Engineering measures (dams, reservoirs, canalization, dykes, and flow regulation) can

39 significantly alter the flow regime of rivers, and reduce the direct relationship with landscape  
40 conditions in the (upper) catchment (Poff et al., 1997). The life expectancy of such structures  
41 depends, however, on the sediment load of incoming rivers and thus on upper watershed conditions  
42 (Graf et al., 2010). Where 'flow regulation' has been included in efforts to assess an economic value  
43 of ecosystem services, it can emerge as a major component of overall value; the economic damage  
44 of floods to cities build on floodplains can be huge and the benefits of avoiding disasters thus large  
45 (Farber et al., 2002; Turner and Daily, 2002; Brauman et al., 2007). The 'counterfactual' part of any  
46 avoided damage argument, however, depends on metrics that are transparent in their basic concept  
47 and relationship with observables. Basic requirements for a metric to be used in managing issues of  
48 public concern in a complex multistakeholder environment are that it i) has a direct relationship with  
49 a problem that needs to be solved ('salience'), ii) is aligned with current science-based  
50 understanding of how the underpinning systems function and can be managed ('credibility') and iii)  
51 can be understood from local and public/policy perspectives ('legitimacy') (Clark et al. 2011). Figure  
52 1 summarizes these requirements, building on van Noordwijk et al. (2016).

53       ⇒ Figure 1

54 In the popular discussion on floods, especially in the tropics, a direct relationship with deforestation  
55 and reforestation is still commonly perceived to dominate, and forest cover is seen as salient and  
56 legitimate metric of watershed quality (or of urgency of restoration where it is low). A requirement  
57 for 30% forest cover, is for example included in the spatial planning law in Indonesia in this context  
58 (Galudra and Sirait, 2009). Yet, rivers are probably dominated by the other 70% of the landscape.  
59 There is a problem with the credibility of assumed deforestation-flood relations (van Noordwijk et  
60 al., 2007; Verbist et al., 2010), beyond the local scales (< 10 km<sup>2</sup>) of paired catchments where ample  
61 direct empirical proof exists, especially in non-tropical climate zones (Bruijnzeel, 1990, 2004).  
62 Current watershed rehabilitation programs that focus on increasing tree cover in upper watersheds  
63 are only partly aligned with current scientific evidence of effects of large-scale tree planting on  
64 streamflow (Ghimire et al., 2014; Malmer et al., 2010; Palmer, 2009; van Noordwijk et al., 2015a).  
65 The relationship between floods and change in forest quality and quantity, and the availability of  
66 evidence for such a relationship at various scales has been widely discussed over the past decades  
67 (Andréassian, 2004; Bruijnzeel, 2004; Bradshaw et al., 2007; van Dijk et al., 2009). Measurements in  
68 Cote d'Ivoire, for example, showed strong scale dependence of runoff from 30-50% of rainfall at 1  
69 m<sup>2</sup> point scale, to 4% at 130 ha watershed scale, linked to spatial variability of soil properties plus  
70 variations in rainfall patterns (Van de Giesen et al., 2000). The ratio between peak and average flow  
71 decreases from headwater streams to main rivers in a predictable manner; while mean annual  
72 discharge scales with (area)<sup>1.0</sup>, maximum river flow was found to scale with (area)<sup>0.4</sup> to (area)<sup>0.7</sup> on  
73 average (Rodríguez-Iturbe and Rinaldo, 2001; van Noordwijk et al., 1998; Herschy, 2002), with even  
74 lower powers for area in flash floods that are linked to an extreme rainfall event over a restricted  
75 area (Marchi et al., 2010). The determinants of peak flow are thus scale-dependent, with space-time  
76 correlations in rainfall interacting with subcatchment-level flow buffering at any point along the  
77 river. Whether and where peak flows lead to flooding depends on the capacity of the rivers to pass  
78 on peak flows towards downstream lakes or the sea, assisted by riparian buffer areas with sufficient  
79 storage capacity (Baldassarre et al., 2013). Reducing local flooding risk by increased drainage  
80 increases flooding risk downstream, challenging the nested-scales management of watersheds to  
81 find an optimal spatial distribution, rather than minimization, of flooding probabilities. Well-studied  
82 effects of forest conversion on peak flows in small upper stream catchments (Bruijnzeel, 2004;

83 Change, 2006; Alila et al., 2009) do not necessarily translate to flooding downstream. With most of  
84 the published studies still referring to the temperate zone, the situation in the tropics (generally in  
85 the absence of snow) is contested (Bonell and Bruijnzeel, 2005). As summarized by Beck et al. (2013)  
86 meso- to macroscale catchment studies (>1 and >10 000 km<sup>2</sup>, respectively) in the tropics, subtropics,  
87 and warm temperate regions have mostly failed to demonstrate a clear relationship between river  
88 flow and change in forest area. Lack of evidence cannot be firmly interpreted as evidence for lack of  
89 effect, however. Detectability of effects depends on their relative size, the accuracy of the  
90 measurement devices, length of observation period, and background variability of the signal. A  
91 recent econometric study for Peninsular Malaysia by Tan-Soo et al. (2014) concluded that, after  
92 appropriate corrections for space-time correlates in the data-set for 31 meso- and macroscale basins  
93 (554-28,643 km<sup>2</sup>), conversion of inland rain forest to monocultural plantations of oil palm or rubber  
94 increased the number of flooding days reported, but not the number of flood events, while  
95 conversion of wetland forests to urban areas reduced downstream flood duration. This Malaysian  
96 study may be the first credible empirical evidence at this scale. The difference between results for  
97 flood duration and flood frequency and the result for draining wetland forests warrant further  
98 scrutiny. Consistency of these findings with river flow models based on a water balance and likely  
99 pathways of water under the influence of change in land cover and land use has yet to be shown.  
100 Two recent studies for Southern China confirm the conventional perspective that deforestation  
101 increases high flows, but are contrasting in effects of Reforestation. Zhou et al. (2010) analysed a 50-  
102 year data set for Guangdong Province in China and concluded that forest recovery had not changed  
103 the annual water yield (or its underpinning water balance terms precipitation and  
104 evapotranspiration), but had a statistically significant positive effect on dry season (low) flows. Liu  
105 et al. (2015), however, found for the Meijiang watershed (6983 km<sup>2</sup>) in subtropical China that while  
106 historical deforestation had decreased the magnitudes of low flows (daily flows  $\leq$  Q95%) by 30.1%,  
107 low flows were not significantly improved by Reforestation. They concluded that recovery of low  
108 flows by Reforestation may take much longer time than expected probably because of severe soil  
109 erosion and resultant loss of soil infiltration capacity after deforestation. Changes in river flow  
110 patterns over a limited period of time can be the combined and interactive effects of variations in  
111 the local rainfall regime, land cover effects on soil structure and engineering modifications of water  
112 flow that can be teased apart with modelling tools (Ma et al., 2014).

113 Lacombe et al. (2015) documented that the hydrological effects of natural regeneration differ from  
114 those of plantation forestry, while forest statistics do not normally differentiate between these  
115 different land covers. In a regression study of the high and low flow regimes in the Volta and  
116 Mekong river basins Lacombe and McCartney (2016) found that in the variation among tributaries  
117 various aspects of land cover and land cover change had explanatory power. Between the two  
118 basins, however, these aspects differed. In the Mekong basin variation in forest cover had no direct  
119 effect on flows, but extending paddy areas resulted in a decrease in downstream low flows, probably  
120 by increasing evapotranspiration in the dry season. In the Volta River Basin, the conversion of forests  
121 to crops (or a reduction of tree cover in the existing parkland system) induced greater downstream  
122 flood flows. This observation is aligned with the experimental identification of an optimal,  
123 intermediate tree cover from the perspective of groundwater recharge in parklands in Burkina Faso  
124 (Ilstedt et al., 2016).

125 The statistical challenges of attribution of cause and effect in such data-sets are considerable with  
126 land use/land cover effects interacting with spatially and temporally variable rainfall, geological

127 configuration and the fact that land use is not changing in random fashion or following any pre-  
128 randomized design (Alila et al., 2009; Rudel et al., 2005). Hydrological analysis across 12 catchments  
129 in Puerto Rico by Beck et al. (2013) did not find significant relationships between the change in  
130 forest cover or urban area, and change in various flow characteristics, despite indications that  
131 regrowing forests increased evapotranspiration.

132 These observations imply that percent tree cover (or other forest related indicators) is probably not  
133 a good metric for judging the ecosystem services provided by a watershed (of different levels of  
134 'health'), and that a metric more directly reflecting changes in river flow may be needed. Here we  
135 will explore a simple recursive model of river flow (van Noordwijk et al., 2011) that (i) is focused on  
136 (loss of) flow predictability, (ii) can account for the types of results obtained by the cited recent  
137 Malaysian study (Tan-Soo et al., 2014), and (iii) may constitute a suitable performance indicator to  
138 monitor watershed 'health' through time.

139 Before discussing the credibility dimension of river flow metrics, the way these relate to the salience  
140 and legitimacy issues around 'flood damage' as policy issue need attention. The salient issue of  
141 'flood damage' is compatible with a common dissection of risk as the product of exposure, hazard  
142 and vulnerability (steps 1, 2 and 3 in Figure 2). Many aspects beyond forests and tree cover play a  
143 role; in fact these factors are multiple steps away (step 7A) from the direct river flow dynamics that  
144 determine floods. Extreme discharge events plus river-level engineering (steps 4 and 5) co-  
145 determine hazard (step 2), while exposure (step 1) depends on topographic position interacting with  
146 human presence, and vulnerability can be modified by engineering at a finer scale and be further  
147 reduced by advice to leave an area in high-risk periods. A recent study (Jongman et al., 2015) found  
148 that human fatalities and material losses between 1980 and 2010 expressed as a share of the  
149 exposed population and gross domestic product were decreasing with rising income. The planning  
150 needed to avoid extensive damage requires quantification of the risk of higher than usual  
151 discharges, especially at the upper tail end of the flow frequency distribution.

152 ⇒ Figure 2

153 The statistical scarcity, per definition, of 'extreme events' and the challenge of data collection where  
154 they do occur, make it hard to rely on site-specific empirical data as such. Inference of risks needs  
155 some trust in extrapolation methods, as is often provided by use of trusted underlying mechanisms  
156 and/or data obtained in a geographical proximity. Existing data on flood frequency and duration, as  
157 well as human and economic damage are influenced by topography, soils, human population density  
158 and economic activity, responding to engineered infrastructure (step 5 in Figure 2), as well as the  
159 extreme rainfall events that are their proximate cause (step 6). Subsidence due to groundwater  
160 extraction in urban areas of high population density is a specific problem for a number of cities built  
161 on floodplains (such as Jakarta and Bangkok), but subsidence of drained peat areas has also been  
162 found to increase flooding risks elsewhere (Sumarga et al., 2016). Common hydrological analysis of  
163 flood frequency (called 1 in 10-, 1 in 100-, 1 in 1000-year flood events, for example) relies on direct  
164 observations at step 4 in Fig. 2, but typically requires spatial extrapolation beyond points of data  
165 collection through river flow models that combine at least steps 5 and 6. Relatively simple ways of  
166 including the conditions in the watershed (step 7) in such models rely on the runoff curve number  
167 method (Ponce et al., 1996) and the SWAT (Soil water assessment tool) model that was built on its  
168 foundation (Gassman et al. 2007). Applications on tropical soils have had mixed success (Oliveira et  
169 al. 2016). Describing peak flows as a proportion of the rainfall event that triggered them has a long

170 history, but where the proportionality factors are estimated for ungauged catchments results may  
171 be unreliable (Efstratiadis et al., 2014). More refined descriptions of the infiltration process (step  
172 7B) are available, using recursive models as filters on empirical data (Grimaldi et al., 2013), but data  
173 for this approach may not be generally available. According to van der Putte et al. (2013) the Green-  
174 Ampt infiltration equation can be fitted to data for dry conditions when soil crusts limit infiltration,  
175 but not in wet winter conditions. These authors argued that simpler models may be better.

176 Analysis of likely change in flood frequencies in the context of climate change adaptation has been  
177 challenging (Milly et al., 2002; Ma et al., 2014). There is a lack of simple performance indicators for  
178 watershed health at its point of relating precipitation P and river flow Q (step 4 in Figure 2) that align  
179 with local observations of river behaviour and concerns about its change and that can reconcile  
180 local, public/policy and scientific knowledge, thereby helping negotiated change in watershed  
181 management (Leimona et al., 2015). The behaviour of rivers depends on many climatic (step 6 in  
182 Figure 2) and terrain factors (step 7A-D in Figure 2) that make it a challenge to differentiate between  
183 human induced ecosystem structural change and soil degradation (step 7B) on one hand and  
184 intrinsic variability on the other. Step 8 in Figure 2 represents the direct influence of climate on  
185 vegetation, but also a possible reverse influence (van Noordwijk et al., 2015b). Hydrological models  
186 tend to focus on predicting hydrographs at one or more temporal scales, and are usually tested on  
187 data-sets from limited locations. Despite many decades (if not centuries) of hydrological modelling,  
188 current hydrologic theory, models and empirical methods have been found to be largely inadequate  
189 for sound predictions in ungauged basins (Hrachowitz et al., 2013). Efforts to resolve this through  
190 harmonization of modelling strategies have so far failed. Existing models differ in the number of  
191 explanatory variables and parameters they use, but are generally dependent on empirical data of  
192 rainfall that are available for specific measurement points but not at the spatial resolution that is  
193 required for a close match between measured and modelled river flow. Spatially explicit models  
194 have conceptual appeal (Ma et al., 2010) but have too many degrees of freedom and too many  
195 opportunities for getting right answers for wrong reasons if used for empirical calibration (Beven,  
196 2011). Parsimonious, parameter-sparse models are appropriate for the level of evidence available to  
197 constrain them, but these parameters are themselves implicitly influenced by many aspects of  
198 existing and changing features of the watershed, making it hard to use such models for scenario  
199 studies of changing land use and change in climate forcing. Here we present a more direct approach  
200 deriving a metric of flow predictability that can bridge local concerns and concepts to quantified  
201 hydrologic function: the 'flow persistence' parameter as directly observable characteristic (step 4 in  
202 Figure 2), that can be logically linked to the primary points of intervention in watershed  
203 management, interacting with climate and engineering-based change.

204 In this contribution to the debate we will first define the metric 'flow persistence' in the context of  
205 temporal autocorrelation of river flow and then derive a way to estimate its numerical value. In part  
206 II we will apply the algorithm to river flow data for a number of contrasting meso-scale watersheds.  
207 In the discussion of this paper we will consider the new flow persistence metric in terms of three  
208 groups of criteria for usable knowledge (Fig. 1; Clark et al., 2011; Lusiana et al., 2011; Leimona et al.,  
209 2015) based on salience (I,II), credibility (III, IV) and legitimacy (V-VII):

- 210 I. Does flow persistence relate to important aspects of watershed behaviour, complementing  
211 existing metrics such as the 'flashiness index' and 'base flow separation' techniques?
- 212 II. Does its quantification help to select management actions?

- 213 III. Is there consistency of numerical results?
- 214 IV. How sensitive is it to bias and random error in data sources?
- 215 V. Does it match local knowledge?
- 216 VI. Can it be used to empower local stakeholders of watershed management?
- 217 VII. Can it inform local risk management?

## 218 **2 Flow persistence in water balance equations**

### 219 **2.1 Recursive model**

220 One of the easiest-to-observe aspects of a river is its day-to-day fluctuation in water level, related to  
 221 the volumetric flow (discharge) via rating curves (Maidment, 1992). Without knowing details of  
 222 upstream rainfall and the pathways the rain takes to reach the river, observation of the daily  
 223 fluctuations in water level allows important inferences to be made. It is also of direct utility: sudden  
 224 rises can lead to floods without sufficient warning, while rapid decline makes water utilization  
 225 difficult. Indeed, a common local description of watershed degradation is that rivers become more  
 226 ‘flashy’ and less predictable, having lost a buffer or ‘sponge’ effect (Joshi et al., 2004; Ranieri et al.,  
 227 2004; Rahayu et al., 2013). A simple model of river flow at time  $t$ ,  $Q_t$ , is that it is similar to that of the  
 228 day before ( $Q_{t-1}$ ), multiplied with  $F_p$ , a dimensionless parameter called ‘flow persistence’ (van  
 229 Noordwijk et al., 2011) plus an additional stochastic term  $Q_{a,t}$ :

$$230 \quad Q_t = F_p Q_{t-1} + Q_{a,t} \quad [1].$$

231  $Q_t$  is for this analysis expressed in  $\text{mm d}^{-1}$ , which means that measurements in  $\text{m}^3 \text{s}^{-1}$  need to be  
 232 divided by the relevant catchment area, with appropriate unit conversion. If river flow were  
 233 constant, it would be perfectly predictable, i.e.  $F_p$  would be 1.0 and  $Q_{a,t}$  zero; in contrast, an  $F_p$ -value  
 234 equal to zero and  $Q_{a,t}$  directly reflecting erratic rainfall represents the lowest possible level of  
 235 predictability.

236 The  $F_p$  parameter is conceptually identical to the ‘recession constant’ commonly used in hydrological  
 237 models, typically assessed during an extended dry period when the  $Q_{a,t}$  term is negligible and  
 238 streamflow consists of base flow only (Tallaksen, 1995); empirical deviations from a straight line in a  
 239 plot of the logarithm of  $Q$  against time are common and point to multiple rather than a single  
 240 groundwater pool that contributes to base flow. The larger catchment area has a possibility to get  
 241 additional flow from multiple independent groundwater contribution.

242 As we will demonstrate in a next section, it is possible to derive  $F_p$  even when  $Q_{a,t}$  is not negligible. In  
 243 climates without distinct dry season this is essential; elsewhere it allows a comparison of apparent  $F_p$   
 244 between wet and dry parts of the hydrologic year. A possible interpretation, to be further explored,  
 245 is that decrease over the years of  $F_p$  indicates ‘watershed degradation’ (i.e. greater contrast between  
 246 high and low flows), and an increase ‘improvement’ or ‘rehabilitation’ (i.e. more stable flows).

247 If we consider the sum of river flow over a period of time (from 1 to  $T$ ) we obtain

$$248 \quad \sum_1^T Q_t = F_p \sum_1^T Q_{t-1} + \sum_1^T Q_{a,t} \quad [2].$$

249 If the period is sufficiently long period for  $Q_T$  minus  $Q_0$  (the values of  $Q_t$  for  $t=T$  and  $t=0$ , respectively)  
 250 to be negligibly small relative to the sum over all  $t$ 's, we may equate  $\sum_1^T Q_t$  with  $\sum_1^T Q_{t-1}$  and obtain a  
 251 first way of estimating the  $F_p$  value:

$$252 \quad F_p = 1 - \sum_1^T Q_{a,t} / \sum_1^T Q_t \quad [3].$$

253 The stochastic  $Q_{a,t}$  can be interpreted in terms of what hydrologists call 'effective rainfall' (i.e. rainfall  
 254 minus on-site evapotranspiration, assessed over a preceding time period  $t_x$  since previous rain  
 255 event):

$$256 \quad Q_t = F_p Q_{t-1} + (1-F_p)(P_{t_x} - E_{t_x}) \quad [4].$$

257 Where  $P_{t_x}$  is the (spatially weighted) precipitation on day  $t$  (or preceding precipitation released as  
 258 snowmelt on day  $t$ ) in  $\text{mm d}^{-1}$ ;  $E_{t_x}$ , also in  $\text{mm d}^{-1}$ , is the preceding evapotranspiration that allowed  
 259 for infiltration during this rainfall event (i.e. evapotranspiration since the previous soil-replenishing  
 260 rainfall that induced empty pore space in the soil for infiltration and retention), or replenishment of  
 261 a water film on aboveground biomass that will subsequently evaporate. More complex attributions  
 262 are possible, aligning with the groundwater replenishing bypass flow and the water isotopic  
 263 fractionation involved in evaporation (Evaristo et al., 2015).

264 The consistency of multiplying effective rainfall with  $(1-F_p)$  can be checked by considering the  
 265 geometric series  $(1-F_p)$ ,  $(1-F_p) F_p$ ,  $(1-F_p) F_p^2$ , ...,  $(1-F_p) F_p^n$  which adds up to  $(1-F_p)(1 - F_p^n)/(1-F_p)$  or  $1 -$   
 266  $F_p^n$ . This approaches 1 for large  $n$ , suggesting that all of the water attributed to time  $t$ , i.e.  $P_t - E_{t_x}$ ,  
 267 will eventually emerge as river flow. For  $F_p = 0$  all of  $(P_t - E_{t_x})$  emerges on the first day, and river flow  
 268 is as unpredictable as precipitation itself. For  $F_p = 1$  all of  $(P_t - E_{t_x})$  contributes to the stable daily flow  
 269 rate, and it takes an infinitely long period of time for the last drop of water to get to the river. For  
 270 declining  $F_p$ , ( $1 > F_p > 0$ ), river flow gradually becomes less predictable, because a greater part of the  
 271 stochastic precipitation term contributes to variable rather than evened-out river flow.

272 Taking long term summations of the right- and left- hand sides of Eq.(4) we obtain:

$$273 \quad \sum Q_t = \sum (F_p Q_{t-1} + (1-F_p)(P_t - E_{t_x})) = F_p \sum Q_{t-1} + (1-F_p)(\sum P_t - \sum E_{t_x}) \quad [5].$$

274 Which is consistent with the basic water budget,  $\sum Q = \sum P - \sum E$ , at time scales long enough for  
 275 changes in soil water buffer stocks to be ignored. As such the total annual, and hence the mean daily  
 276 river flow are independent of  $F_p$ . This does not preclude that processes of watershed degradation or  
 277 restoration that affect the partitioning of  $P$  over  $Q$  and  $E$  also affect  $F_p$ .

## 278 **2.2 Base flow**

279 Clarifying the  $Q_a$  contribution is equivalent with one of several ways to separate base flow from peak  
 280 flows. Rearranging Eq.(3) we obtain

$$281 \quad \sum_1^T Q_{a,t} = (1 - F_p) \sum_1^T Q_t \quad [6].$$

282 The  $\sum Q_{a,t}$  term reflects the sum of peak flows in mm. Its complement,  $F_p \sum Q_t$ , reflects the sum of base  
 283 flow, also in mm. For  $F_p = 1$  (the theoretical maximum) we conclude that all  $Q_{a,t}$  must be zero, and all  
 284 flow is 'base flow'.

## 285 2.3 Low flows

286 The lowest flow expected in an annual cycle is  $Q_x F_p^{N_{max}}$  where  $Q_x$  is flow on the first day without rain  
287 and  $N_{max}$  the longest series of dry days. Taken at face value, a decrease in  $F_p$  has a strong effect on  
288 low-flows, with a flow of 10% of  $Q_x$  reached after 45, 22, 14, 10, 8 and 6 days for  $F_p = 0.95, 0.9, 0.85,$   
289  $0.8, 0.75$  and  $0.7$ , respectively. However, the groundwater reservoir that is drained, equalling the  
290 cumulative dry season flow if the dry period is sufficiently long, is  $Q_x/(1-F_p)$ . If  $F_p$  decreases to  $F_{px}$  but  
291 the groundwater reservoir ( $Res = Q_x/(1-F_p)$ ) is not affected, initial flows in the dry period will be  
292 higher ( $Q_x F_{px}^i (1-F_{px}) Res > Q_x F_p^i (1-F_p) Res$  for  $i < \log((1-F_{px})/(1-F_p))/\log(F_p/F_{px})$ ). It thus matters how  
293 low flows are evaluated: from the perspective of the lowest level reached, or as cumulative flow.  
294 The combination of climate, geology and land form are the primary determinants of cumulative low  
295 flows, but if land cover reduces the recharge of groundwater there may be impacts on dry season  
296 flow, that are not directly reflected in  $F_p$ .

297 If a single  $F_p$  value would account for both dry and wet season, the effects of changing  $F_p$  on low  
298 flows may well be more pronounced than those on flood risk. Empirical tests are needed of the  
299 dependence of  $F_p$  on  $Q$  (see below). Analysis of the way an aggregate  $F_p$  depends on the dominant  
300 flow pathways provides a basis for differentiating  $F_p$  within a hydrologic year.

301

## 302 2.4 Flow-pathway dependence of flow persistence

303 The patch-level partitioning of water between infiltration and overland flow is further modified at  
304 hillslope level, with a common distinction between three pathways that reach streams: overland  
305 flow, interflow and groundwater flow (Band et al., 1993; Weiler and McDonnell, 2004). An additional  
306 interpretation of Eq.(1), potentially adding to our understanding of results but not needed for  
307 analysis of empirical data, can be that three pathways of water through a landscape contribute to  
308 river flow (Barnes, 1939): groundwater release with  $F_{p,g}$  values close to 1.0, overland flow with  $F_{p,o}$   
309 values close to 0, and interflow with intermediate  $F_{p,i}$  values.

$$310 Q_t = F_{p,g} Q_{t-1,g} + F_{p,i} Q_{t-1,i} + F_{p,o} Q_{t-1,o} + Q_{a,t} \quad [7],$$

$$311 F_p = (F_{p,g} Q_{t-1,g} + F_{p,i} Q_{t-1,i} + F_{p,o} Q_{t-1,o})/Q_{t-1} \quad [8].$$

312 On this basis a decline or increase in overall weighted average  $F_p$  can be interpreted as indicator of a  
313 shift of dominant runoff pathways through time within the watershed. Dry season flows are  
314 dominated by  $F_{p,g}$ . The effective  $F_p$  in the rainy season can be interpreted as indicating the relative  
315 importance of the other two flow pathways.  $F_p$  reflects the fractions of total river flow that are based  
316 on groundwater, overland flow and interflow pathways:

$$317 F_p = F_{p,g} (\sum Q_{t,g} / \sum Q_t) + F_{p,o} (\sum Q_{t,o} / \sum Q_t) + F_{p,i} (\sum Q_{t,i} / \sum Q_t) \quad [9].$$

318 Beyond the type of degradation of the watershed that, mostly through soil compaction, leads to  
 319 enhanced infiltration-excess (or Hortonian) overland flow (Delfs et al., 2009), saturated conditions  
 320 throughout the soil profile may also induce overland flow, especially near valley bottoms (Bonell,  
 321 1993; Bruijnzeel, 2004). Thus, the value of  $F_{p,o}$  can be substantially above zero if the rainfall has a  
 322 significant temporal autocorrelation, with heavy rainfall on subsequent days being more likely than  
 323 would be expected from general rainfall frequencies. If rainfall following a wet day is more likely to  
 324 occur than following a dry day, as is commonly observed in Markov chain analysis of rainfall patterns  
 325 (Jones and Thornton, 1997; Bardossy and Plate, 1991), the overland flow component of total flow  
 326 will also have a partial temporal autocorrelation, adding to the overall predictability of river flow. In  
 327 a hypothetical climate with evenly distributed rainfall, we can expect  $F_p$  to be 1.0 even if there is no  
 328 infiltration and the only pathway available is overland flow. Even with rainfall that is variable at any  
 329 point of observation but has low spatial correlation it is possible to obtain  $F_p$  values of (close to) 1.0  
 330 in a situation with (mostly) overland flow (Ranieri et al., 2004).

### 331 **2.5 Relationship between flow persistence and flashiness index**

332 The Richards-Baker 'R-B Flashiness index' (Baker et al. 2004) is defined as

$$333 \quad FI = \frac{\sum_t |\Delta Q_t|}{\sum_t Q_t} = \frac{\sum_{ti} (Q_t - Q_{t-1}) + \sum_{td} (Q_{t-1} - Q_t)}{\sum_t Q_t} \quad [10]$$

334 with  $ti$  indicating all times  $t$  that  $Q_t > Q_{t-1}$  and  $td$  indicating all times  $t$  that  $Q_t < Q_{t-1}$ . Over a  
 335 timeframe that flow has no net trend, the sum of increments ( $\sum_{ti} (Q_t - Q_{t-1})$ ) is equal to the sum of  
 336 declines ( $\sum_{td} (Q_{t-1} - Q_t)$ ).

337 Substituting equation [5] in [10] we obtain:

$$338 \quad FI = \frac{2(1-F_p)(0.5 \Delta S + \sum_{ti} (P_t - E_{tx} - Q_t))}{\sum_t Q_t} = \frac{2(1-F_p)(-0.5 \Delta S + \sum_{td} (-P_t + E_{tx} + Q_t))}{\sum_t Q_t} \quad [11]$$

339 With  $\Delta S$  representing change in catchment storage;  $\Delta S = (1-F_p) (-\sum_{ti} (P_t - E_{tx} - Q_t) + \sum_{td} (-P_t + E_{tx} + Q_t))$ .

340 This suggests that  $FI = 2(1-F_p)$  is a first approximation and becomes zero for  $F_p = 1$ . These  
 341 approximations require that changes in the catchment have no influence on  $P_t$  or  $E_{tx}$  values. If  $E_{tx}$  is  
 342 negatively affected (either by a change in vegetation or by insufficient buffering, reducing water  
 343 availability on non-rainfall days) flashiness will increase, beyond the main effects on  $F_p$ .

344 The rainfall term, counted positive for all days with flow increase and negatively for days with  
 345 declining flow, hints at one of the major reasons why the flashiness index tends to get smaller when  
 346 larger catchment areas are involved: rainfall will tend to get more evenly distributed over time,  
 347 unless the spatial correlation of rainfall is (close to) 1 and all rainfall derives from fronts passing over  
 348 the area uniformly. Where (part of) precipitation occurs as snow, the timing of snow melt defines  $P_t$   
 349 as used here. Where vegetation influences timing and synchrony of snowmelt, this will be reflected  
 350 in the flashiness index. It may not directly influence flow persistence, but will be accounted for in the  
 351 flow description that uses flow persistence as key parameter.

### 352 3. Methods

#### 353 3.1 River flow data for four tropical watersheds

354 To test the applicability of the  $F_p$  metric and explore its properties, data from four Southeast Asian  
355 watersheds were used, that will be described and further analysed in part II. The first watershed  
356 data set is the Way Besai (414.4 km<sup>2</sup>) in Lampung province, Sumatra, Indonesia (Verbist et al., 2010).  
357 With an elevation between 720-1831 m a.s.l., the Way Besai is dominated by various coffee  
358 production systems (64%), with remaining forest (18%), horticulture and crops (12%) and other land  
359 uses (6%). Daily rainfall data from 1976 – 2007, was generated by interpolation of eight rainfall  
360 stations using Thiessen polygons; data were obtained from BMKG (*Agency on Meteorology,*  
361 *Climatology and Geophysics*), PU (Public Work Agency) and PLN (*National Electricity Company*). The  
362 average of annual rainfall was 2474 mm, with observed values in the range 1216 – 3277 mm. River  
363 flow data at the outflow of the Way Besai was also obtained from PU and PUSAIR (*Centre for*  
364 *Research and Development on Water Resources*), with an average of river flow of 16.7 m<sup>3</sup>/s.

365 Data from three other watersheds were used to explore the variation of  $F_p$  across multiple years and  
366 its relationship with the Flashiness Index: Bialo (111.7 km<sup>2</sup>) in South Sulawesi, Indonesia with  
367 Agroforestry as the dominant land cover type, Cidanau (241.6 km<sup>2</sup>) in West Java, Indonesia,  
368 dominated by mixed Agroforestry land uses but with a peat swamp before the final outlet and Mae  
369 Chaem (3892 km<sup>2</sup>) in Northern Thailand, part of the upper Ping Basin, and dominated by evergreen,  
370 deciduous and pine forest. Detailed information on these watersheds and the data sources is  
371 provided in Paper II.

#### 372 3.2 Numerical examples

373 For ‘Monte Carlo’ simulations a river flow model representing equation [1] was implemented in a  
374 spreadsheet model that is available from the authors on request. Fixed values for  $F_p$  were used in  
375 combination with a stochastic  $Q_{a,t}$  value. The latter was obtained from a random generator (rand)  
376 with two settings for a (truncated) sinus-based daily rainfall probability: A) one for situations that  
377 have approximately 120 rainy days, and an annual  $Q$  of around 1600 mm, and B) one that leads to  
378 around 45 rainy days and an annual total around 600 mm. Maximum daily  $Q_{a,t}$  was chosen as 60 mm  
379 in both cases. For the figures, realizations for various  $F_p$  values were retained that were within 10%  
380 of this number of rainy days and annual flow total, to focus on the effects of  $F_p$  as such.

#### 381 3.3 Flow persistence as a simple flood risk indicator

382 For numerical examples (implemented in a spreadsheet model) flow on each day can be derived as:

$$383 Q_t = \sum_j^t F_p^{t-j} (1-F_p) p_j P_j \quad [12].$$

384 Where  $p_j$  reflects the occurrence of rain on day  $j$  (reflecting a truncated sine distribution for seasonal  
385 trends) and  $P_j$  is the rain depth (drawn from a uniform distribution). From this model the effects of  $F_p$   
386 (and hence of changes in  $F_p$ ) on maximum daily flow rates, plus maximum flow totals assessed over a  
387 2-5 d period, was obtained in a Monte Carlo process (without Markov autocorrelation of rainfall in  
388 the default case – see below). Relative flood protection was calculated as the difference between  
389 peak flows (assessed for 1-5 d duration after a 1 year ‘warm-up’ period) for a given  $F_p$  versus those  
390 for  $F_p = 0$ , relative to those at  $F_p = 0$ .

391 **3.4 An algorithm for deriving  $F_p$  from a time series of stream flow data**

392 Equation (3) provides a first method to derive  $F_p$  from empirical data if these cover a full hydrologic  
393 year. In situations where there is no complete hydrograph and/or in situations where we want to  
394 quantify  $F_p$  for shorter time periods (e.g. to characterise intraseasonal flow patterns) and the change  
395 in the storage term of the water budget equation cannot be ignored, we need an algorithm for  
396 estimating  $F_p$  from a series of daily  $Q_t$  observations.

397 Where rainfall has clear seasonality, it is attractive and indeed common practice to derive a  
398 groundwater recession rate from a semi-logarithmic plot of  $Q$  against time (Tallaksen, 1995). As we  
399 can assume for such periods that  $Q_{a,t} = 0$ , we obtain  $F_p = Q_t / Q_{t-1}$ , under these circumstances. We  
400 cannot be sure, however, that this  $F_{p,g}$  estimate also applies in the rainy season, because overall wet-  
401 season  $F_p$  will include contributions by  $F_{p,o}$  and  $F_{p,i}$  as well (compare Eq. 9). In locations without a  
402 distinct dry season, we need an alternative method.

403 A biplot of  $Q_t$  against  $Q_{t-1}$  will lead to a scatter of points above a line with slope  $F_p$ , with points above  
404 the line reflecting the contributions of  $Q_{a,t} > 0$ , while the points that plot on the  $F_p$  line itself  
405 represent  $Q_{a,t} = 0 \text{ mm d}^{-1}$ . There is no independent source of information on the frequency at which  
406  $Q_{a,t} = 0$ , nor what the statistical distribution of  $Q_{a,t}$  values is if it is non-zero. Calculating back from the  
407  $Q_t$  series we can obtain an estimate ( $Q_{a,Fptry}$ ) of  $Q_{a,t}$  for any given estimate ( $F_{p,try}$ ) of  $F_p$ , and select the  
408 most plausible  $F_p$  value. For high  $F_{p,try}$  estimates there will be many negative  $Q_{a,Fptry}$  values, for low  
409  $F_{p,try}$  estimates all  $Q_{a,Fptry}$  values will be larger. An algorithm to derive a plausible  $F_p$  estimate can thus  
410 make use of the corresponding distribution of ‘apparent  $Q_a$ ’ values as estimates of  $F_{p,try}$ , calculated  
411 as  $Q_{a,Fptry} = Q_t - F_{p,try} Q_{t-1}$ . While  $Q_{a,t}$  cannot be negative in theory, small negative  $Q_a$  estimates are  
412 likely when using real-world data with their inherent errors. The FlowPer  $F_p$  algorithm (van  
413 Noordwijk et al., 2011) derives the distribution of  $Q_{a,Fptry}$  estimates for a range of  $F_{p,try}$  values (Figure  
414 3B) and selects the value  $F_{p,try}$  that minimizes the variance  $\text{Var}(Q_{a,Fptry})$  (or its standard deviation)  
415 (Figure 3C). It is implemented in a spreadsheet workbook that can be downloaded from the ICRAF  
416 website (<http://www.worldagroforestry.org/output/flowper-flow-persistence-model>)

417 → Figure 3

418 A consistency test is needed that the high-end  $Q_t$  values relate to  $Q_{t+1}$  in the same way as do low or  
419 medium  $Q_t$  values. Visual inspection of  $Q_{t+1}$  versus  $Q_t$ , with the derived  $F_p$  value, provides a  
420 qualitative view of the validity of this assumption. The  $F_p$  algorithm can be applied to any population  
421 of  $(Q_{t-1}, Q_t)$  pairs, e.g. selected from a multiyear data set on the basis of 3-month periods within the  
422 hydrological year.

423 **3.5 Flashiness and flow separation**

424 Hydrographs analysed for  $F_p$  were also used for calculating the Richards-Baker or R-B Flashiness  
425 index (Baker et al. 2004) by summing the absolute values of all daily changes in flow. Two common  
426 flow separation algorithms (fixed and sliding interval methods, Furey and Gupta, 2001) were used to  
427 estimate the base flow fraction at an annual basis. The average of the two was compared to  $F_p$ .

428 **4 Results**

429 **4.1 Numerical examples**

430 Figure 4 provides two examples, for annual river flows of around 1600 and 600 mm  $y^{-1}$ , of the way a  
431 change in  $F_p$  values (based on Eq. 1) influences the pattern of river flow for a unimodal rainfall  
432 regime with a well-developed dry season. The increasing 'spikiness' of the graph as  $F_p$  is lowered,  
433 regardless of annual flow, indicates reduced predictability of flow on any given day during the wet  
434 season on the basis of the flow on the preceding day.

435       ⇒ Figure 4

436 A bi-plot of river flow on subsequent days for the same simulations (Figure 5) shows two main  
437 effects of reducing the  $F_p$  value: the scatter increases, and the slope of the lower envelope  
438 containing the swarm of points is lowered (as it equals  $F_p$ ). Both of these changes can provide entry  
439 points for an algorithm to estimate  $F_p$  from empirical time series, provided the basic assumptions of  
440 the simple model apply and the data are of acceptable quality.

441       ⇒ Figure 5

442 For the numerical examples shown in Figure 4, the relative increase of the maximum daily flow when  
443 the  $F_p$  value decreased from a value close to 1 (0.98) to nearly 0 depended on the rainfall regime;  
444 with lower annual rainfall but the same maximum daily rainfall, the response of peak flows to  
445 decrease in  $F_p$  became stronger.

446 **4.2 Flood intensity and duration**

447 Figure 6 shows the effect of  $F_p$  values in the range 0 to 1 on the maximum flows obtained with a  
448 random time series of 'effective rainfall', compared to results for  $F_p = 0$ . Maximum flows were  
449 considered at time scales of 1 to 5 days, in a moving average routine. This way a relative flood  
450 protection, expressed as reduction of peak flow, could be related to  $F_p$  (Figure 6A).

451       ⇒ Figure 6

452 Relative flood protection rapidly decreased from its theoretical value of 100% at  $F_p = 1$  (when there  
453 was no variation in river flow), to less than 10% at  $F_p$  values of around 0.5. Relative flood protection  
454 was slightly lower when the assessment period was increased from 1 to 5 days (between 1 and 3 d it  
455 decreased by 6.2%, from 3 to 5 d by a further 1.3%). Two counteracting effects are at play here: a  
456 lower  $F_p$  means that a larger fraction ( $1-F_p$ ) of the effective rainfall contributes to river flow, but the  
457 increased flow is less persistent. In the example the flood protection in situations where the rainfall  
458 during 1 or 2 d causes the peak is slightly stronger than where the cumulative rainfall over 3-5 d  
459 causes floods, as typically occurs downstream.

460 As we expect from equation 5 that peak flow is to  $(1-F_p)$  times peak rainfall amounts, the effect of a  
461 change in  $F_p$  not only depends on the change in  $F_p$  that we are considering, but also on its initial  
462 value. Higher initial  $F_p$  values will lead to more rapid increases in high flows for the same reduction in  
463  $F_p$  (Figure 6B). However, flood duration rather responds to changes in  $F_p$  in a curvilinear manner, as  
464 flow persistence implies flood persistence (once flooding occurs), but the greater the flow  
465 persistence the less likely such a flooding threshold is passed (Figure 6C). The combined effect may  
466 be restricted to about 3 d of increase in flood duration for the parameter values used in the default  
467 example, but for different parametrization of the stochastic  $\epsilon$  other results might be obtained.

### 468 **4.3 Algorithm for $F_p$ estimates from river flow time series**

469 The algorithm has so far returned non-ambiguous  $F_p$  estimates on any modelled time series data of  
470 river flow, as well as for all empirical data set we tested (including all examples tested in part II),  
471 although there probably are data sets on which it can breakdown. Visual inspection of  $Q_{t-1}/Q_t$  biplots  
472 (as in Figure 4) can provide clues to non-homogenous data sets, to potential situations where  
473 effective  $F_p$  depends on flow level  $Q_t$  and where data are not consistent with a straight-line lower  
474 envelope. Where river flow estimates were derived from a model with random elements, however,  
475 variation in  $F_p$  estimates was observed, that suggests that specific aspects of actual rainfall, beyond  
476 the basic characteristics of a watershed and its vegetation, do have at least some effect. Such effects  
477 deserve to be further explored for a set of case studies, as their strength probably depends on  
478 context.

### 479 **4.4 Flow persistence compared to base flow and flashiness index**

480 Figure 7 compares results for a hydrograph of a single year for the Way Besai catchment, described  
481 in more detail in paper II. While there is agreement on most of what is indicated as baseflow, the  
482 short term response to peaks in the flow differ, with baseflow in the  $F_p$  method more rapidly  
483 increasing after peak events.

484       ⇒ Figure 7

485 When compared across multiple years for four Southeast Asian catchments (figure 8), there is partial  
486 agreement in the way interannual variation is described in each catchment, while numerical values  
487 are similar. However, the ratio of what is indicated as baseflow according to the  $F_p$  method and  
488 according to standard hydrograph separation varies from 1.05 to 0.86.

489       ⇒ Figure 8

490 Figure 9 compares numerical results for the R-B Flashiness Index with  $F_p$  for the four test catchments  
491 and for a number of hydrographs constructed as in Fig. 3A. The two concepts are inversely related,  
492 as expected from equation [11], but where  $F_p$  is constrained to the 0-1 interval, the R-B Flashiness  
493 Index can attain values up to 2.0, with the value for  $F_p = 0$  depending on properties of the local  
494 rainfall regime. Where hydrographs were generated with a simple flow model with  $F_p$  parameter as  
495 key variable, the flashiness index is more tightly related to, especially for higher  $F_p$  values, than  
496 where both flashiness index and  $F_p$  were derived from existing flow data (Figure 9B versus 9A). The  
497 difference in slope between the four watersheds in Fig. 9A appears to be primarily related to aspects  
498 of the local rainfall pattern that deserve further analysis in larger data sets of this nature.

499       ⇒ Figure 9

500

## 501 **5 Discussion**

502 We will discuss the flow persistence metric based on the seven questions raised from the  
503 perspectives of salience, credibility and legitimacy and refer back to figure 2 that clarified how  
504 ecosystem structure, ecosystem function and human land use interact in causal loops that can lead  
505 to flood damage, its control and/or prevention.

506 **5.1 Saliience**

507 Key *saliience* aspects are “Does flow persistence relate to important aspects of watershed  
508 behaviour?” and “Does it help to select management actions?”. A major finding in the derivation of  
509  $F_p$  was that the flow persistence measured at daily time scale can be logically linked to the long-term  
510 water balance under the assumption that the watershed is defined on the basis of actual  
511 groundwater flows, and that the proportion of peak rainfall that translates to peak river flow equals  
512 the complement of flow persistence. This feature links effects on floods of changes in watershed  
513 quality, as commonly expressed in curve numbers and flashiness indices, to effects on low flows, as  
514 commonly expressed in base flow metrics. The  $F_p$  parameter as such does not predict when and  
515 where flooding will occur, but it does help to assess to what extent another condition of the  
516 watershed, with either higher or lower  $F_p$  would translate the same rainfall into larger or small peak  
517 water flows. This is salient, especially if the relative contributions of (anthropogenic) land cover and  
518 the (exogenous, probabilistic) specifics of the rainfall pattern can be further teased apart (see part  
519 II). Where  $F_p$  may describe the descending branch of hydrographs at a relevant time scale, details of  
520 the ascending branch beyond the maximum daily flow reached may be relevant for reducing flood  
521 damage, and may require more detailed study at higher temporal resolution.

522 Figures 3 and 6 show that most of the effects of a decreasing  $F_p$  value on peak discharge (which is  
523 the basis for downstream flooding) occur between  $F_p$  values of 1 and 0.7, with the relative flood  
524 protection value reduced to 10% when  $F_p$  reaches 0.5. As indicated in Figure 2, peak discharge is only  
525 one of the factors contributing to flood risk in terms of human casualties and physical damage. Flood  
526 risks are themselves nonlinearly and in strongly topography-specific ways related to the volume of  
527 river flow after extreme rainfall events. While the expected fraction of rainfall that contributes to  
528 direct flow is linearly related to rainfall via  $(1-F_p)$ , flooding risk as such will have a non-linear  
529 relationship with rainfall, that depends on topography and antecedent rainfall. Catchment changes,  
530 such as increases or decreases in percentage tree cover, will generally have a non-linear relationship  
531 with  $F_p$  as well as with flooding risks. The  $F_p$  value has an inverse effect on the fraction of recent  
532 rainfall that becomes river flow, but the effect on peak flows is less, as higher  $F_p$  values imply higher  
533 base flow. The way these counteracting effects balance out depends on details of the local rainfall  
534 pattern (including its Markov chain temporal autocorrelation), as well as the downstream  
535 topography and risk of people being at the wrong time at a given place, but the  $F_p$  value is an  
536 efficient way of summarizing complex land use mosaics and upstream topography in its effect on  
537 river flow. The difference between wet-season and dry-season  $F_p$  deserves further analysis. In  
538 climates with a real rainless dry-season, dry season  $F_p$  is dominated by the groundwater release  
539 fraction of the watershed, regardless of land cover, while in wet season it depends on the mix  
540 (weighted average) of flow pathways. The degree to which  $F_p$  can be influenced by land cover needs  
541 to be assessed for each landscape and land cover combination, including the locally relevant forest  
542 and forest derived land classes, with their effects on interception, soil infiltration and time pattern of  
543 transpiration. The  $F_p$  value can summarize results of models that explore land use change scenarios  
544 in local context. To select the specific management actions that will maintain or increase  $F_p$  a locally  
545 calibrated land use/hydrology model is needed, such as GenRiver (part II), DHV (Bergström, 1995) or  
546 SWAT (Yen et al., 2015).

547 The “health” wording has been used as a comprehensive concept of the way a) climate forcing, b)  
548 watershed vegetation and soil conditions and c) engineering interventions interact on functional

549 aspects of river flow. Ma et al (2014) described a method to separate these three influences on river  
550 flow. In the four catchments we used as example there have been no major dams or reservoirs  
551 installed upstream of the points of measurement. Where these do exist the specific operating rules  
552 of reservoirs need to be included in any model and these can have a major influence on downstream  
553 flow, depending on the primary use for power generation, dry season irrigation or stabilizing river  
554 flow for riverine transport. Although a higher  $F_p$  value will in most cases be desirable (and a decrease  
555 in  $F_p$  undesirable), we may expect that In an ecological perspective on watershed health, the change  
556 in low flows that can occur in the flow regime of degrading and intensively managed watersheds  
557 alike, depending on the management rules for reservoirs, is at least as relevant as changes in flood  
558 risks, as many aquatic organisms thrive during floods (Pahl-Wostl et al., 2013; Poff et al., 2010).  
559 Downstream biota can be expected to have adapted to the pre-human flow conditions, inherent  $F_p$   
560 and variability. Decreased variability of flow achieved by engineering interventions (e.g. a reservoir  
561 with constant release of water to generate hydropower) may have negative consequences for fish  
562 and other biota (Richter et al., 2003; McCluney et al., 2014). In an extensive literature review Poff  
563 and Zimmerman (2010) found no general, transferable quantitative relationships between flow  
564 alteration and ecological response, but the risk of ecological change increases with increasing  
565 magnitude of flow alteration.

566 Various geographically defined watershed health concepts are in use (see for example  
567 <https://www.epa.gov/hwp/healthy-watersheds-projects-region-5>; City of Fort Collins, 2015,  
568 employing a range of specific indicators, including the 'R-B flashiness index' (Baker et al. 2004). The  
569 definition of watershed health, like that of human health has evolved over time. Human health was  
570 seen as a state of normal function that could be disrupted from time to time by disease. In 1948 the  
571 World Health Organization (1958) proposed a definition that aimed higher, linking health to well-  
572 being, in terms of physical, mental, and social aspects, and not merely the absence of disease and  
573 infirmity. Health became seen as the ability to maintain homeostasis and recover from injury, but  
574 remained embedded in the environment in which humans function.

## 575 **5.2 Credibility**

576 Key *credibility* questions are "Consistency of numerical results?" and "How sensitive are results to  
577 bias and random error in data sources?". A key strength of our flow persistence parameter, that it  
578 can be derived from a limited number of observations of river flow at a single point along the river,  
579 without knowledge of rainfall events and catchment conditions, is also its major weakness. If rainfall  
580 data exist, and especially rainfall data that apply to each subcatchment, the  $Q_a$  term doesn't have to  
581 be treated as a random variable and event-specific information on the flow pathways may be  
582 inferred for a more precise account of the hydrograph. But for the vast majority of rivers in the  
583 tropics, advances in remotely sensed rainfall data are needed to achieve that situation and  $F_p$  may be  
584 all that is available to inform public debates on the location-specific relation between forests and  
585 floods.

586 The main conclusions from the numerical examples analysed so far are that intra-annual variability  
587 of  $F_p$  values between wet and dry seasons was around 0.2, interannual variability in either annual or  
588 seasonal  $F_p$  was generally in the 0.1 range, while the difference between observed and simulated  
589 flow data as basis for  $F_p$  calculations was mostly less than 0.1. With current methods, it seems that  
590 effects of land cover change on flow persistence that shift the  $F_p$  value by about 0.1 are the limit of

591 what can be asserted from empirical data (with shifts of that order in a single year a warning sign  
592 rather than a firmly established change). When derived from observed river flow data  $F_p$  is suitable  
593 for monitoring change (degradation, restoration) and can be a serious candidate for monitoring  
594 performance in outcome-based ecosystem service management contracts. In interpreting changes in  
595  $F_p$  as caused by changes in the condition in the watershed, however, changes in specific properties of  
596 the rainfall regime must be excluded. At the scale of paired catchment studies this assumption may  
597 be reasonable, but in temporal change (or using specific events as starting point for analysis), it is  
598 not easy to disentangle interacting effects (Ma et al., 2014). Recent evidence that vegetation not  
599 only responds to, but also influences rainfall (arrow 10 in Figure 2; van Noordwijk et al., 2015b)  
600 further complicates the analysis across scales.

601 As indicated, the  $F_p$  method is related to earlier methods used in streamflow hydrograph separation  
602 of base flow and quick flow. While textbooks (Ward and Robinson, 2000; Hornberger et al 2014)  
603 tend to be critical of the lack of objectivity of graphical methods, algorithms are used for deriving the  
604 minimum flow in a fixed or sliding period of reference as base flow (Sloto and Crouse, 1996; Furey  
605 and Gupta, 2001). The time interval used for deriving the minimum flow depends on catchment size.

606 Recursive models that describe flow in a next time interval on the basis of a fraction of that in the  
607 preceding time interval with a term for additional flow due to additional rainfall have been used in  
608 analysis of peak flow event before, with time intervals as short as 1 minute rather than the 1 day we  
609 use here (Rose, 2004). Through reference to an overall mass balance a relationship similar to what  
610 we found here ( $F_p$  times preceding flow plus  $1 - F_p$  times recent inputs) was also used in such  
611 models. To our knowledge, the method we describe here at daily timescales has not been used  
612 before.

613 The idea that the form of the storage-discharge function can be estimated from analysis of  
614 streamflow fluctuations has been explored before for a class of catchments in which discharge is  
615 determined by the volume of water in storage (Kirchner, 2009). Such catchments behave as simple  
616 first-order nonlinear dynamical systems and can be characterized in a single-equation rainfall-runoff  
617 model that predicted streamflow, in a test catchment in Wales, as accurately as other models that  
618 are much more highly parameterized. This model of the  $dQ/dt$  versus  $Q$  relationship can also be  
619 analytically inverted; thus, it can, according to Kirchner (2009), be used to “do hydrology backward,”  
620 that is, to infer time series of whole-catchment precipitation directly from fluctuations in  
621 streamflow. The slope of the log-log relationship between flow recession ( $dQ/dt$ ) and  $Q$  that  
622 Kirchner (2009) used is conceptually similar to the  $F_p$  metric we derived here, but the specific  
623 algorithm to derive the parameter from empirical data differs. Further exploration of the underlying  
624 assumptions is needed. Estimates of  $dQ/dt$  are sensitive to noise in the measurement of  $Q$  and the  
625 possibly frequent and small increases in  $Q$  can be separated from the expected flow recession in the  
626 algorithm we presented here.

627 Table 1 compares a number of properties (Saliency and Legitimacy in properties 1-4, Credibility  
628 dimensions in 5-10) for the R-B Flashiness Index (Baker et al. 2004) and flow persistence. The main  
629 advantage of continuing with the flashiness index is that there is an empirical basis for comparisons  
630 and the index has been included in existing ‘watershed health’ monitoring programs, especially in  
631 the USA. The main advantage of including  $F_p$  is that it can be estimated from incomplete flow  
632 records, has a clear link to peak flow events and has a more direct relationship with underlying flow  
633 pathways, changes in rainfall (or snowmelt) and evapotranspiration, reflecting land cover change.

634 → Table 1

635 Seifert and Beven (2009) discussed the increase in predictive skill of models depending on the  
636 amount of location-specific data that can be used to constrain them. They found that the ensemble  
637 prediction of multiple models for a single location clearly outperformed the predictions using single  
638 parameter sets and that surprisingly little runoff data was necessary to identify model  
639 parameterizations that provided good results for ‘ungauged’ test periods in cases where actual  
640 measurements were available. Their results indicated that a few runoff measurements can contain  
641 much of the information content of continuous runoff time series. The way these conclusions might  
642 be modified if continuous measurements for limited time periods, rather than separated single data  
643 points on river flow could be used, remains to be explored. Their study indicated that results may  
644 differ significantly between catchments and critical tests of  $F_p$  across multiple situations are  
645 obviously needed, as paper II will provide.

646 In discussions and models of temperate zone hydrology (Bergström, 1995; Seifert, 1999) snowmelt is  
647 a major component of river flow and effects of forest cover on spring temperatures are important to  
648 the buffering of the annual peaks in flow that tend to occur in this season. Application of the  $F_p$   
649 method to data describing such events has yet to be done.

### 650 **5.3 Legitimacy**

651 *Legitimacy* aspects are “Does it match local knowledge?” and “Can it be used to empower local  
652 stakeholders of watershed management?” and “Can it inform risk management?”. As the  $F_p$   
653 parameter captures the predictability of river flow that is a key aspect of degradation according to  
654 local knowledge systems, its results are much easier to convey than full hydrographs or exceedance  
655 probabilities of flood levels. By focusing on observable effects at river level, rather than prescriptive  
656 recipes for land cover (“Reforestation”), the  $F_p$  parameter can be used to more effectively compare  
657 the combined effects of land cover change, changes in the riparian wetlands and engineered water  
658 storage reservoirs, in their effect on flow buffering. It is a candidate for shifting environmental  
659 service reward contracts from input to outcome based monitoring (van Noordwijk et al., 2012). As  
660 such it can be used as part of a negotiation support approach to natural resources management in  
661 which levelling off on knowledge and joint fact finding in blame attribution are key steps to  
662 negotiated solutions that are legitimate and seen to be so (van Noordwijk et al., 2013; Leimona et  
663 al., 2015). Quantification of  $F_p$  can help assess tactical management options (Burt et al., 2014) as in a  
664 recent suggestion to minimize negative downstream impacts of forestry operations on stream flow  
665 by avoiding land clearing and planting operations in locally wet La Niña years. But the most  
666 challenging aspect of the management of flood, as any other environmental risk, is that the  
667 frequency of disasters is too low to intuitively influence human behaviour where short-term risk  
668 taking benefits are attractive. Wider social pressure is needed for investment in watershed health  
669 (as a type of insurance premium) to be mainstreamed, as individuals waiting to see evidence of  
670 necessity are too late to respond. In terms of flooding risk, actions to restore or retain watershed  
671 health can be similarly justified as insurance premium. It remains to be seen whether or not the  
672 transparency of the  $F_p$  metric and its intuitive appeal are sufficient to make the case in public debate  
673 when opportunity costs of foregoing reductions in flow buffering by profitable land use are to be  
674 compensated and shared (Burt et al., 2014).

## 675 **5.4 Conclusions and specific questions for a set of case studies**

676 In conclusion, the  $F_p$  metric appears to allow an efficient way of summarizing complex landscape  
677 processes into a single parameter that reflects the effects of landscape management within the  
678 context of the local climate. If rainfall patterns change but the landscape does not, the resultant flow  
679 patterns may reflect a change in watershed health (van Noordwijk et al., 2016). Flow persistence is  
680 the result of rainfall persistence and the temporal delay provided by the pathway water takes  
681 through the soil and the river system. High flow persistence indicates a reliable water supply, while  
682 minimizing peak flow events. Wider tests of the  $F_p$  metric as boundary object in science-practice-  
683 policy boundary chains (Kirchhoff et al., 2015; Leimona et al., 2015) are needed. Further tests for  
684 specific case studies can clarify how changes in tree cover (deforestation, reforestation and  
685 agroforestation) in different contexts influence river flow dynamics and  $F_p$  values. Sensitivity to  
686 specific realizations of underlying time-space rainfall patterns needs to be quantified, before  
687 changes in  $F_p$  can be attributed to changed 'watershed health', rather than chance events.

## 688 **Data availability**

689 The algorithm used is freely available. Specific data used in the case studies are explained and  
690 accounted for in Part II.

## 691 **Author contributions**

692 Meine van Noordwijk designed method and paper, Lisa Tanika refined the empirical algorithm and  
693 handled the case study data and modelling for part II, and Betha Lusiana contributed statistical  
694 analysis; all contributed and approved the final manuscript

## 695 **Acknowledgements**

696 This research is part of the Forests, Trees and Agroforestry research program of the CGIAR. Several  
697 colleagues contributed to the development and early tests of the  $F_p$  method. Thanks are due to Eike  
698 Luedeling, Sonya Dewi, Sampurno Bruijnzeel and three anonymous reviewers for comments on an  
699 earlier version of the manuscript.

## 700 **References**

- 701 Alila, Y., Kura, P.K., Schnorbus, M., and Hudson, R.: Forests and floods: A new paradigm sheds light  
702 on age-old controversies, *Water Resour. Res.*, 45, W08416, 2009.
- 703 Andréassian, V.: Waters and forests: from historical controversy to scientific debate, *Journal of*  
704 *Hydrology*, 291, 1–27, 2004.
- 705 Baker, D.B., Richards, R.P., Loftus, T.T. and Kramer, J.W.: A new flashiness index: Characteristics and  
706 applications to midwestern rivers and streams. *Journal of the American Water Resources*  
707 *Association*, Paper No. 03095, 2004.
- 708 Baldassarre, G.D., Kooy, M., Kemerink, J.S., and Brandimarte, L.: Towards understanding the dynamic  
709 behaviour of floodplains as human-water systems, *Hydrology and Earth System Sciences*, 17(8),  
710 3235-3244, 2013.
- 711 Bardossy, A. and Plate, E.J.: Modeling daily rainfall using a semi-Markov representation of  
712 circulation pattern occurrence, *Journal of Hydrology*, 122(1), 33-47, 1991.

713 Band, L.E., Patterson, P., Nemani, R., and Running, S.W.: Forest ecosystem processes at the  
714 watershed scale: incorporating hillslope hydrology, *Agricultural and Forest Meteorology*, 63(1-2),  
715 93-126, 1993.

716 Barnes, B.S.: The structure of discharge-recession curves, *Eos, Transactions American Geophysical*  
717 *Union*, 20(4), 721-725, 1939.

718 Beck, H. E., Bruijnzeel, L. A., Van Dijk, A. I. J. M., McVicar, T. R., Scatena, F. N., and Schellekens, J.: The  
719 impact of forest regeneration on streamflow in 12 mesoscale humid tropical  
720 catchments, *Hydrology and Earth System Sciences* ,17(7), 2613-2635, 2013.

721 Bergström, S.: The HBV model. In: Singh, V.P., (Ed.), *Computer Models of Watershed Hydrology*, Ch.  
722 13, pp. 443-476, Water Resources Publications, Highlands Ranch, Colorado, USA, 1130 pp., 1995.

723 Beven, K.J.: *Rainfall-runoff modelling: the primer*, John Wiley & Sons, 2011

724 Bishop, J. and Pagiola, S. (Eds.): *Selling forest environmental services: market-based mechanisms for*  
725 *conservation and development*, Taylor & Francis, Abingdon (UK), 2012.

726 Bonell, M.: Progress in the understanding of runoff generation dynamics in forests, *Journal of*  
727 *Hydrology*, 150, 217-275, 1993.

728 Bonell, M. and Bruijnzeel, L.A. (eds.): *Forests, water and people in the humid tropics: past, present*  
729 *and future hydrological research for integrated land and water management*. Cambridge  
730 University Press, Cambridge (UK), 2005.

731 Bradshaw, C.J.A., Sodhi, N.S., Peh, K.S.H., and Brook, B.W.: Global evidence that deforestation  
732 amplifies flood risk and severity in the developing world, *Global Change Biol*, 13, 2379–2395,  
733 2007.

734 Brauman, K.A., Daily, G.C., Duarte, T.K.E., and Mooney, H.A.: The nature and value of ecosystem  
735 services: an overview highlighting hydrologic services, *Annu. Rev. Environ. Resour.*, 32, 67-98,  
736 2007.

737 Bruijnzeel, L.A.: *Hydrology of Moist Tropical Forests and Effects of Conversion: a State of Knowledge*  
738 *Review*. IHP-UNESCO Humid Tropical Programme, Paris, 224 pp, 1990.

739 Bruijnzeel, L.A.: Hydrological functions of tropical forests: not seeing the soil for the trees, *Agr.*  
740 *Ecosyst. Environ.*, 104, 185–228, 2004.

741 Burt, T.P., Howden, N.J.K., McDonnell, J.J., Jones, J.A., and Hancock, G.R.: Seeing the climate through  
742 the trees: observing climate and forestry impacts on streamflow using a 60-year record,  
743 *Hydrological Processes*, doi: 10.1002/hyp.10406, 2014.

744 City of Fort Collins, *River Health Assessment Framework la Poudre River*.  
745 <http://www.fcgov.com/naturalareas/pdf/river-health-report-final-appendix.pdf>, 2015.

746 Clark, W. C., Tomich, T. P., van Noordwijk, M., Guston, D., Catacutan, D., Dickson, N. M., and McNie,  
747 E.: Boundary work for sustainable development: natural resource management at the  
748 Consultative Group on International Agricultural Research (CGIAR), *Proc. Nat. Acad. Sci.*,  
749 doi:10.1073/pnas.0900231108, 2011.

750 Delfs, J.O., Park, C.H., and Kolditz, O.: A sensitivity analysis of Hortonian flow, *Advances in Water*  
751 *Resources*. 32(9), 1386-1395, 2009.

752 Efstratiadis, A., Koussis, A.D., Koutsoyiannis, D. and Mamassis, N.: Flood design recipes vs. reality: can  
753 predictions for ungauged basins be trusted? *Natural Hazards and Earth System Sciences*, 14(6), 1417-1428,  
754 2014.

755 Evaristo, J., Jasechko, S., and McDonnell, J.J.: Global separation of plant transpiration from  
756 groundwater and streamflow, *Nature*, 525(7567), 91-94, 2015.

757 Farber, S.C., Costanza, R. and Wilson, M.A.: Economic and ecological concepts for valuing ecosystem  
758 services. *Ecological economics*, 41(3), 375-392, 2002.

759 Furey, P.R. and Gupta, V.K.: A physically based filter for separating base flow from streamflow time  
760 series. *Water Resources Research*, 37(11), 2709-2722, 2001.

761 Galudra, G. and Sirait, M.: A discourse on Dutch colonial forest policy and science in Indonesia at the  
762 beginning of the 20th century. *International Forestry Review* 11(4), 524-533, 2009

763 Gassman, P.W., Reyes, M.R., Green, C.H. and Arnold, J.G.: The soil and water assessment tool: historical  
764 development, applications, and future research directions. *Transactions of the ASABE*, 50(4), 1211-1250,  
765 2007.

766 Graf, W.L., Wohl, E., Sinha, T. and Sabo, J.L., 2010. Sedimentation and sustainability of western American  
767 reservoirs. *Water Resources Research*, 46(12), 2010.

768 Grimaldi, S., Petroselli, A. and Romano, N.: Green-Ampt Curve-Number mixed procedure as an empirical tool  
769 for rainfall-runoff modelling in small and ungauged basins. *Hydrological Processes*, 27(8), 1253-1264,  
770 2013.

771 Ghimire, C.P., Bruijnzeel, L.A., Lubczynski, M.W., and Bonell, M.: Negative trade-off between changes  
772 in vegetation water use and infiltration recovery after reforestation degraded pasture land in the  
773 Nepalese Lesser Himalaya, *Hydrology and Earth System Sciences*, 18(12), 4933-4949, 2014.

774 Herschy, R.W.: The world's maximum observed floods. *Flow Measurement and Instrumentation* 13  
775 (5-6), 231-235, 2002.

776 Hornberger, G.M., Wiberg, P.L., D'Odorico, P. and Raffensperger, J.P.: *Elements of physical*  
777 *hydrology*. John Hopkins University Press, 2014.

778 Hrachowitz, M., Savenije, H.H.G., Blöschl, G., McDonnell, J.J., Sivapalan, M., Pomeroy, J.W.,  
779 Arheimer, B., Blume, T., Clark, M. P., Ehret, U., Fenicia, F., Freer, J E., Gelfan, A., Gupta, H.V.,  
780 Hughes, D. A., Hut, R.W., Montanari, A., Pande, S., Tetzlaff, D., Troch, P.A., Uhlenbrook, S.,  
781 Wagener, T., Winsemius, H.C., Woods, R.A., Zehe, E., and Cudennec, C.: A decade of Predictions  
782 in Ungauged Basins (PUB)—a review, *Hydrological sciences journal*, 58(6), 1198-1255, 2013.

783 Ilstedt, U., Tobella, A.B., Bazié, H.R., Bayala, J., Verbeeten, E., Nyberg, G., Sanou, J., Benegas, L.,  
784 Murdiyarso, D., Laudon, H., and Sheil, D.: Intermediate tree cover can maximize groundwater  
785 recharge in the seasonally dry tropics, *Scientific reports*, 6, 2016

786 Jones, P.G. and Thornton, P.K.: Spatial and temporal variability of rainfall related to a third-order  
787 Markov model, *Agricultural and Forest Meteorology*, 86(1), 127-138, 1997.

- 788 Jongman, B., Winsemius, H. C., Aerts, J. C., de Perez, E. C., van Aalst, M. K., Kron, W., and Ward, P. J.:  
789 Declining vulnerability to river floods and the global benefits of adaptation, In: Proceedings of  
790 the National Academy of Sciences, 112(18), E2271-E2280, 2015.
- 791 Joshi, L., Schalenbourg, W., Johansson, L., Khasanah, N., Stefanus, E., Fagerström, M.H., and van  
792 Noordwijk, M.: Soil and water movement: combining local ecological knowledge with that of  
793 modellers when scaling up from plot to landscape level, In: van Noordwijk, M., Cadisch, G. and  
794 Ong, C.K. (Eds.) *Belowground Interactions in Tropical Agroecosystems*, CAB International,  
795 Wallingford (UK), 349-364, 2004.
- 796 Kirchhoff, C.J., Esselman, R., and Brown, D.: Boundary Organizations to Boundary Chains: Prospects  
797 for Advancing Climate Science Application, *Climate Risk Management*,  
798 doi:10.1016/j.crm.2015.04.001, 2015.
- 799 Kirchner, J.W.: Catchments as simple dynamical systems: Catchment characterization, rainfall-runoff  
800 modeling, and doing hydrology backward. *Water Resources Research*, 45(2).  
801 DOI: 10.1029/2008WR006912, 2009.
- 802 Lacombe, G. and McCartney, M.: Evaluating the flow regulating effects of ecosystems in the Mekong  
803 and Volta river basins, Colombo, Sri Lanka, International Water Management Institute (IWMI)  
804 Research Report 166, doi: 10.5337/2016.202, 2016.
- 805 Lacombe, G., Ribolzi, O., de Rouw, A., Pierret, A., Latsachak, K., Silvera, N., Pham Dinh, R., Orange, D.,  
806 Janeau, J.-L., Souleth, B., Robain, H., Taccon, A., Sengphaathith, P., Mouche, E.,  
807 Sengtaheuanghoung, O., Tran Duc, T., and Valentin, C.: Afforestation by natural regeneration or  
808 by tree planting: Examples of opposite hydrological impacts evidenced by long-term field  
809 monitoring in the humid tropics, *Hydrology and Earth System Sciences Discussions*, 12, 12615-  
810 12648, 2015.
- 811 Leimona, B., Lusiana, B., van Noordwijk, M., Mulyoutami, E., Ekadinata, A., and Amaruzama, S.:  
812 Boundary work: knowledge co-production for negotiating payment for watershed services in  
813 Indonesia, *Ecosystems Services*, 15, 45–62, 2015.
- 814 Liu, W., Wei, X., Fan, H., Guo, X., Liu, Y., Zhang, M., and Li, Q.: Response of flow regimes to  
815 deforestation and reforestation in a rain-dominated large watershed of subtropical  
816 China, *Hydrological Processes*, 29, 5003-5015 , 2015.
- 817 Lusiana, B., van Noordwijk, M., Suyamto, D., Joshi, L., and Cadisch, G.: Users' perspectives on validity  
818 of a simulation model for natural resource management, *International Journal of Agricultural  
819 Sustainability*, 9(2), 364-378, 2011.
- 820 Ma, X., Xu, J. and van Noordwijk, M.: Sensitivity of streamflow from a Himalayan catchment to  
821 plausible changes in land cover and climate, *Hydrological Processes*, 24, 1379–1390, 2010.
- 822 Ma, X., Lu, X., van Noordwijk, M., Li, J.T., and Xu, J.C.: Attribution of climate change, vegetation  
823 restoration, and engineering measures to the reduction of suspended sediment in the Kejie  
824 catchment, southwest China, *Hydrol. Earth Syst. Sci.*, 18, 1979–1994, 2014.
- 825 Maidment, D.R.: *Handbook of hydrology*, McGraw-Hill Inc., 1992.

- 826 Malmer, A., Murdiyarso, D., Bruijnzeel L.A., and Ilstedt, U.: Carbon sequestration in tropical forests  
827 and water: a critical look at the basis for commonly used generalizations, *Global Change*  
828 *Biology*, 16(2), 599-604, 2010.
- 829 Marchi, L., Borga, M., Preciso, E. and Gaume, E.: Characterisation of selected extreme flash floods in Europe  
830 and implications for flood risk management. *Journal of Hydrology*, 394(1), 118-133, 2010.
- 831 McCluney, K.E., Poff, N.L., Palmer, M.A., Thorp, J.H., Poole, G.C., Williams, B.S., Williams, M.R., and  
832 Baron, J.S.: Riverine macrosystems ecology: sensitivity, resistance, and resilience of whole river  
833 basins with human alterations, *Frontiers in Ecology and the Environment*, 12(1), 48-58, 2014.
- 834 Milly, P.C.D., Wetherald, R., Dunne, K.A., and Delworth, T.L.: Increasing risk of great floods in a  
835 changing climate, *Nature*, 415(6871), 514-517, 2002.
- 836 Oliveira, P.T.S., Nearing, M.A., Hawkins, R.H., Stone, J.J., Rodrigues, D.B.B., Panachuki, E. and Wendland, E.:  
837 Curve number estimation from Brazilian Cerrado rainfall and runoff data. *Journal of Soil and Water*  
838 *Conservation*, 71(5), 420-429, 2016
- 839 Pahl-Wostl, C., Arthington, A., Bogardi, J., Bunn, S.E., Hoff, H., Lebel, L., Nikitina, E., Palmer, M., Poff, L.N.,  
840 Richards, K. and Schlüter, M.: Environmental flows and water governance: managing sustainable water  
841 uses. *Current Opinion in Environmental Sustainability*, 5(3), pp.341-351, 2013.
- 842 Palmer, M.A.: Reforming watershed restoration: science in need of application and applications in  
843 need of science, *Estuaries and coasts*, 32(1), 1-17, 2009.
- 844 Poff, N.L. and Zimmerman, J.K.: Ecological responses to altered flow regimes: a literature review to inform the  
845 science and management of environmental flows. *Freshwater Biology*, 55(1), 194-205, 2010.
- 846 Poff, N.L., Allan, J.D., Bain, M.B., Karr, J.R., Prestegard, K.L., Richter, B.D., Sparks, R.E. and Stromberg, J.C.: The  
847 natural flow regime. *BioScience*, 47(11), 769-784, 1997.
- 848 Poff, N.L., Richter, B.D., Arthington, A.H., Bunn, S.E., Naiman, R.J., Kendy, E., Acreman, M., Apse, C., Bledsoe,  
849 B.P., Freeman, M.C. and Henriksen, J.: The ecological limits of hydrologic alteration (ELOHA): a new  
850 framework for developing regional environmental flow standards. *Freshwater Biology*, 55(1), 147-170,  
851 2010
- 852 Ponce, V.M. and Hawkins, R.H.: Runoff curve number: Has it reached maturity? *Journal of Hydrologic*  
853 *Engineering*, 1(1), 11-19, 1996
- 854 Rahayu, S., Widodo, R.H., van Noordwijk, M., Suryadi, I., and Verbist, B.: Water monitoring in  
855 watersheds. Bogor, Indonesia, World Agroforestry Centre (ICRAF) SEA Regional Program,, 2013
- 856 Ranieri, S.B.L., Stirzaker, R., Suprayogo, D., Purwanto, E., de Willigen, P., and van Noordwijk, M.:  
857 Managing movements of water, solutes and soil: from plot to landscape scale. In: van Noordwijk,  
858 M., Cadisch, G. and Ong, C.K. (Eds.) *Belowground Interactions in Tropical Agroecosystems*, CAB  
859 International, Wallingford (UK), 329-347, 2004.
- 860 Richter, B.D., Mathews, R., Harrison, D.L., and Wigington, R.: Ecologically sustainable water  
861 management: managing river flows for ecological integrity, *Ecological applications*, 13(1), 206-  
862 224, 2003.
- 863 Rodríguez-Iturbe, I. and Rinaldo, A.: *Fractal river basins: chance and self-organization*, Cambridge  
864 University Press, Cambridge, 2001.

865 Rose, C.W.: *An introduction to the environmental physics of soil, water and watersheds*. Cambridge  
866 University Press, Cambridge (UK) 2004.

867 Rudel, T. K., Coomes, O. T., Moran, E., Achard, F., Angelsen, A., Xu, J., and Lambin, E.: Forest  
868 transitions: towards a global understanding of land use change, *Global Environmental*  
869 *Change*, 15(1), 23-31, 2005.

870 Seibert, J.: Regionalisation of parameters for a conceptual rainfall-runoff model. *Agricultural and*  
871 *Forest Meteorology* 98-99: 279-293, 1999.

872 Seibert, J., Beven, K.J.: Gauging the ungauged basin: how many discharge measurements are  
873 needed? *Hydrol. Earth Syst. Sci.*, 13, 883–892, 2009

874 Sloto, R.A. and Crouse, M.Y.: *HYSEP, a computer program for streamflow hydrograph separation and*  
875 *analysis*. US Department of the Interior, US Geological Survey, 1996.

876 Sumarga, E., Hein, L., Hooijer, A., and Vernimmen, R.: Hydrological and economic effects of oil palm  
877 cultivation in Indonesian peatlands, *Ecology and Society*, 21(2), 2016.

878 Tallaksen, L.M.: A review of baseflow recession analysis, *J Hydrol*, 165, 349-370, 1995.

879 Tan-Soo, J.S., Adnan, N., Ahmad, I., Pattanayak, S.K., and Vincent, J.R.: Econometric Evidence on  
880 Forest Ecosystem Services: Deforestation and Flooding in Malaysia. *Environmental and Resource*  
881 *Economics*, on-line: <http://link.springer.com/article/10.1007/s10640-014-9834-4>, 2014.

882 Turner, R.K. and Daily, G.C.: The ecosystem services framework and natural capital  
883 conservation. *Environmental and Resource Economics*, 39(1), 25-35, 2008

884 Van de Giesen, N.C., Stomph, T.J., and De Ridder, N.: Scale effects of Hortonian overland flow and  
885 rainfall–runoff dynamics in a West African catena landscape, *Hydrological Processes*, 14,165-  
886 175, 2000.

887 Van den Putte, A., Govers, G., Leys, A., Langhans, C., Clymans, W. and Diels, J.: Estimating the parameters of  
888 the Green–Ampt infiltration equation from rainfall simulation data: Why simpler is better. *Journal of*  
889 *Hydrology*, 476, 332-344, 2013.

890 van Dijk, A.I., van Noordwijk, M., Calder, I.R., Bruijnzeel, L.A., Schellekens, J., and Chappell, N.A.:  
891 Forest-flood relation still tenuous – comment on ‘Global evidence that deforestation amplifies  
892 flood risk and severity in the developing world’, *Global Change Biology*, 15, 110-115, 2009.

893 van Noordwijk, M., van Roode, M., McCallie, E.L., and Lusiana, B.: Erosion and sedimentation as  
894 multiscale, fractal processes: implications for models, experiments and the real world, In: F.  
895 Penning de Vries, F. Agus and J. Kerr (Eds.) *Soil Erosion at Multiple Scales, Principles and*  
896 *Methods for Assessing Causes and Impacts*. CAB International, Wallingford, 223-253, 1998.

897 van Noordwijk, M., Agus, F., Verbist, B., Hairiah, K., and Tomich, T.P.: *Managing Watershed Services*,  
898 In: Scherr, S.J. and McNeely, J.A. (Eds) *Ecoagriculture Landscapes. Farming with Nature: The*  
899 *Science and Practice of Ecoagriculture*, Island Press, Washington DC, 191 – 212, 2007.

900 van Noordwijk, M., Widodo, R.H., Farida, A., Suyamto, D., Lusiana, B., Tanika, L., and Khasanah, N.:  
901 *GenRiver and FlowPer: Generic River and Flow Persistence Models. User Manual Version 2.0.*  
902 Bogor, Indonesia, World Agroforestry Centre (ICRAF) Southeast Asia Regional Program, 2011.

903 van Noordwijk, M., Leimona, B., Jindal, R., Villamor, G.B., Vardhan, M., Namirembe, S., Catacutan, D.,  
904 Kerr, J., Minang, P.A., and Tomich, T.P.: Payments for Environmental Services: evolution towards  
905 efficient and fair incentives for multifunctional landscapes, *Annu. Rev. Environ. Resour.*, 37, 389-  
906 420, 2012.

907 van Noordwijk, M., Lusiana, B., Leimona, B., Dewi, S., and Wulandari, D.: Negotiation-support toolkit  
908 for learning landscapes, Bogor, Indonesia, World Agroforestry Centre (ICRAF) Southeast Asia  
909 Regional Program, 2013.

910 van Noordwijk, M., Leimona, B., Xing, M., Tanika, L., Namirembe, S., and Suprayogo, D.: Water-  
911 focused landscape management. *Climate-Smart Landscapes: Multifunctionality In Practice*. eds  
912 Minang PA et al.. Nairobi, Kenya, World Agroforestry Centre (ICRAF), 179-192, 2015a.

913 van Noordwijk, M., Bruijnzeel, S., Ellison, D., Sheil, D., Morris, C., Gutierrez, V., Cohen, J., Sullivan, C.,  
914 Verbist, B., and Muys, B.: Ecological rainfall infrastructure: investment in trees for sustainable  
915 development, ASB Brief no 47. Nairobi. ASB Partnership for the Tropical Forest Margins, 2015b.

916 van Noordwijk M, Kim Y-S, Leimona B, Hairiah K, Fisher LA,: Metrics of water security, adaptive  
917 capacity and Agroforestry in Indonesia. *Current Opinion on Environmental Sustainability* (in  
918 press: <http://dx.doi.org/10.1016/j.cosust.2016.10.004>), 2016.

919 Verbist, B., Poesen, J., van Noordwijk, M. Widiyanto, Suprayogo, D., Agus, F., and Deckers, J.: Factors  
920 affecting soil loss at plot scale and sediment yield at catchment scale in a tropical volcanic  
921 Agroforestry landscape, *Catena*, 80, 34-46, 2010.

922 Ward, R.C. and Robinson, M.: *Principles of hydrology*. 4<sup>th</sup> edition. New York: McGraw-Hill, 2000.

923 Weiler, M. and McDonnell, J.: Virtual experiments: a new approach for improving process  
924 conceptualization in hillslope hydrology, *Journal of Hydrology*, 285(1), 3-18, 2004

925 Winsemius, H.C., van Beek, L.P.H., Jongman, B., Ward, P.J., and Bouwman, A.: A framework for global  
926 river flood risk assessments, *Hydrol Earth Syst Sci*, 17, 1871–1892, 2013.

927 World Health Organization: The first ten years of the World Health Organization. Geneva: WHO,  
928 1958

929 Yen, H., White, M.J., Jeong, J., Arabi, M. and Arnold, J.G.: Evaluation of alternative surface runoff  
930 accounting procedures using the SWAT model, *International Journal of Agricultural and*  
931 *Biological Engineering*, 8(3), 54-68, 2015.

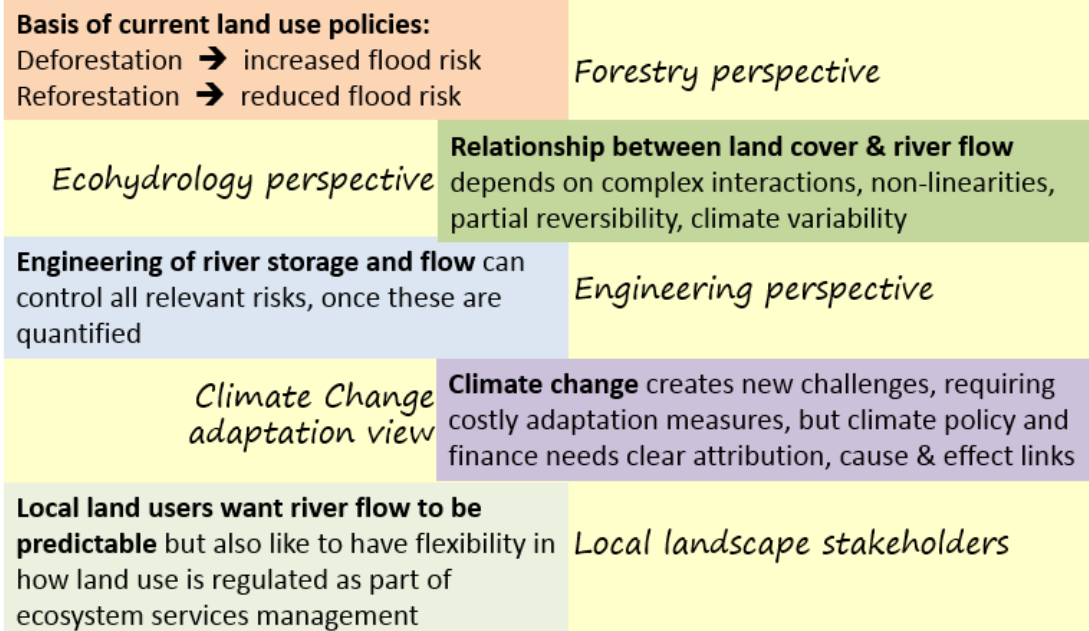
932 Zhou, G., Wei, X., Luo, Y., Zhang, M., Li, Y., Qiao, Y., Liu, H., and Wang, C.: Forest recovery and river  
933 discharge at the regional scale of Guangdong Province, China, *Water Resources Research*, 46(9),  
934 W09503, doi:10.1029/2009WR00829, 2010.

935

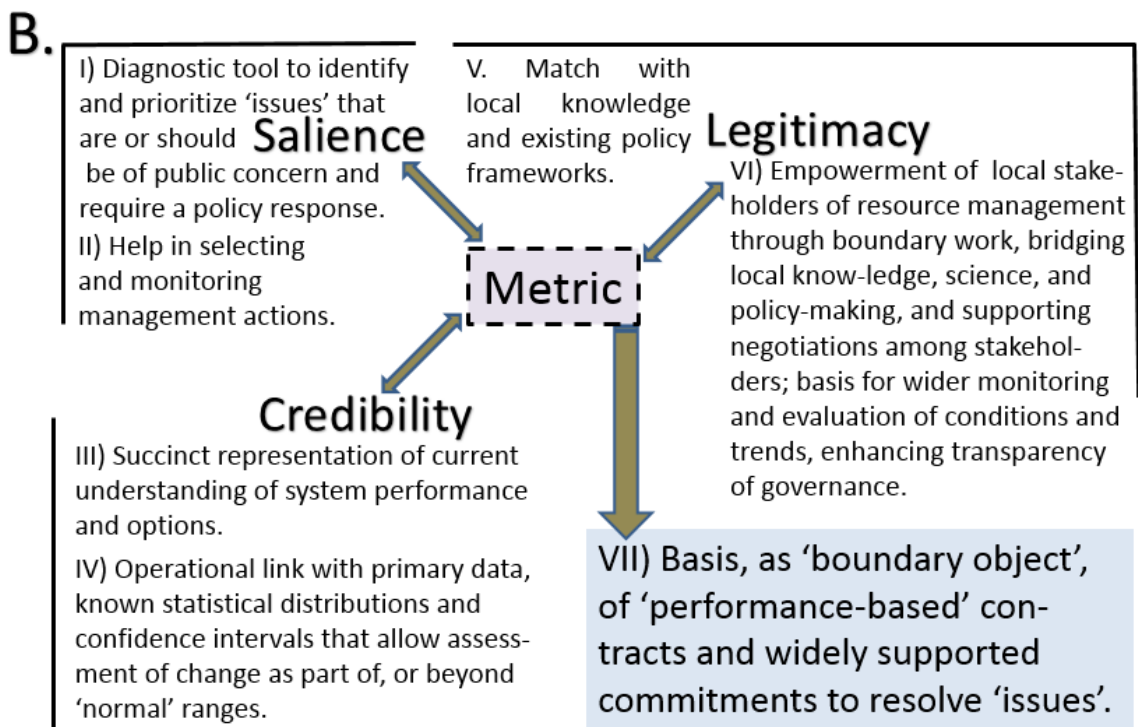
# A. Interests ↔ Understanding ↔ Metrics

multistakeholder resource management processes

→ Monitoring → Diagnosis → Tradeoff analysis → Innovation → Scenarios → Negotiations →

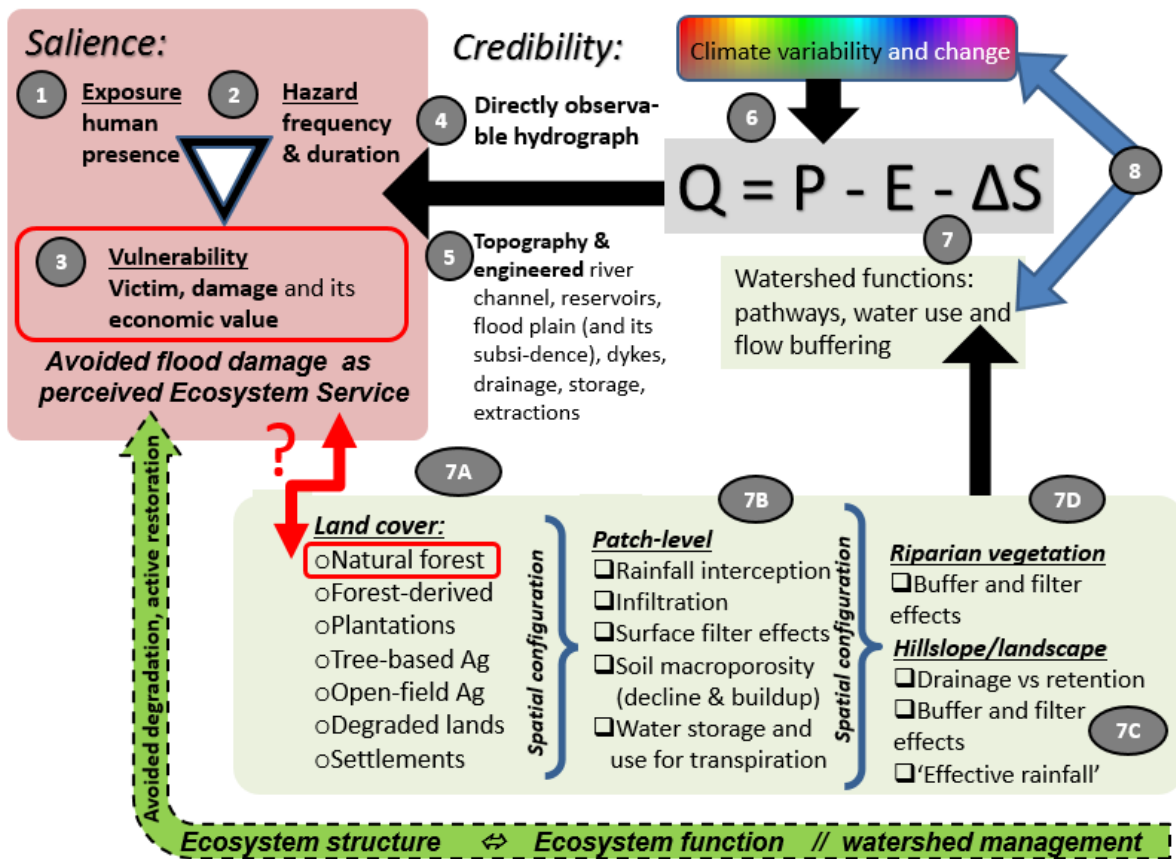


937



938

939 Figure 1. A. Multiple perspectives on the way flood risk is to be understood, monitored and handled  
 940 according to different knowledge systems; B. Basic requirements for a 'metric' to be used in public  
 941 discussions of natural resource management issues that deserve to be resolved and acted upon  
 942 (modified from van Noordwijk et al., 2016)



943

944

945

946

947

948

949

950

951

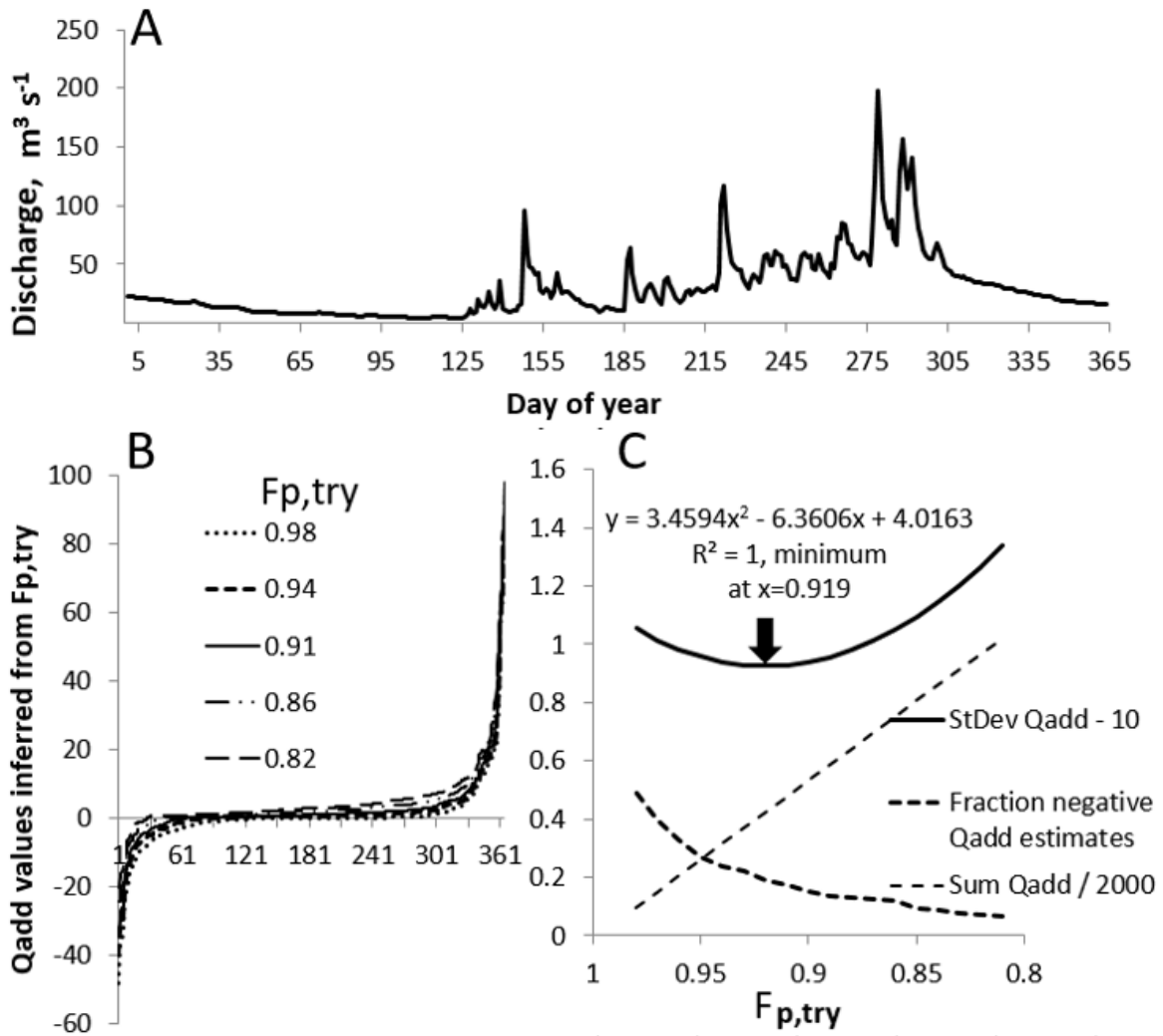
952

953

954

955

Figure 2. Steps in a causal pathway that relates the salience of ‘avoided flood damage as ecosystem service’ to the interaction of exposure (1; being in the wrong place at critical times), hazard (2; spatially explicit flood frequency and duration) and human determinants of vulnerability (3); the hazard component depends, in common scientific analysis, on the pattern of river flow described in a hydrograph (4), which in turn is understood to be influenced by conditions along the river channel (5), precipitation and potential evapotranspiration ( $E_{pot}$  as climatic factors (6) and the condition in the watershed (7) determining evapotranspiration ( $E_{act}$ ), temporary water storage ( $\Delta S$ ) and water partitioning over overland flow and infiltration; these watershed functions in turn depend on the interaction of terrain (topography, soils, geology), vegetation and human land use; current understanding of a two-way interaction between vegetation and rainfall adds further complexity (8)

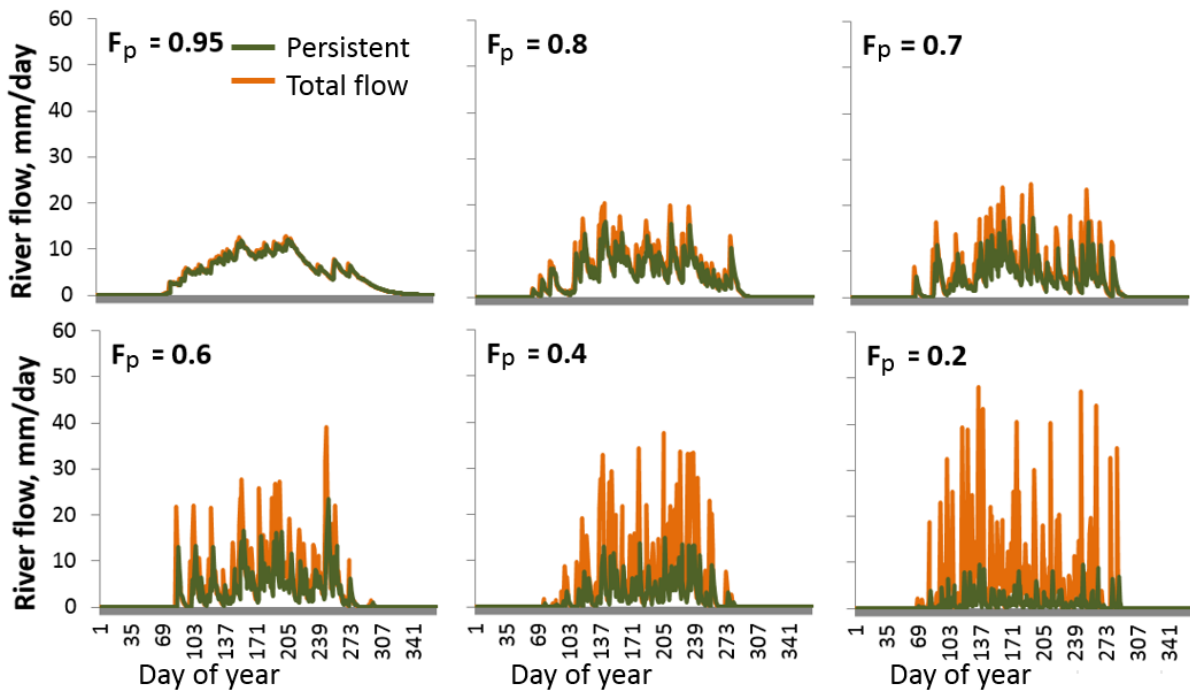


956

957 Figure 3. Example of the derivation of best fitting  $F_{p,try}$  value for an example hydrograph (A) on the  
 958 basis of the inferred  $Q_a$  distribution (cumulative frequency in B), and three properties of this  
 959 distribution (C): its sum, frequency of negative values and standard deviation; the  $F_{p,try}$  minimum  
 960 of the latter is derived from the parameters of a fitted quadratic equation

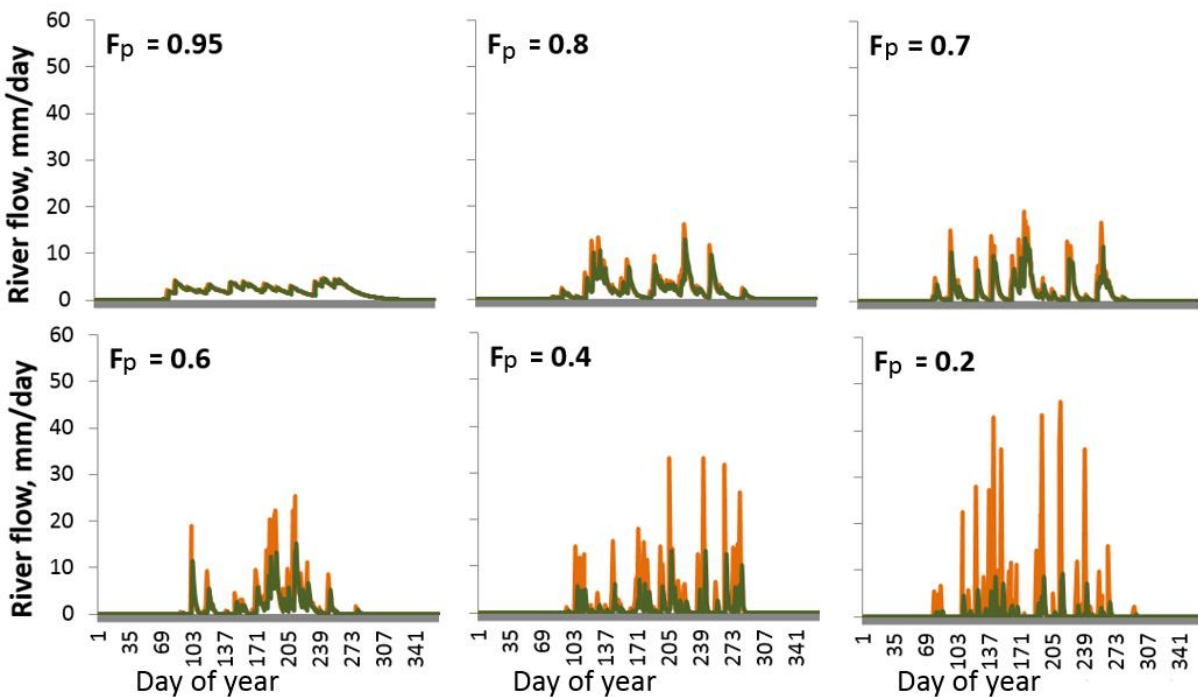
961

**A.** 120 rainy days,  $Q \sim 1600$  mm/yr



962

**B.** 45 rainy days,  $Q \sim 600$  mm/yr



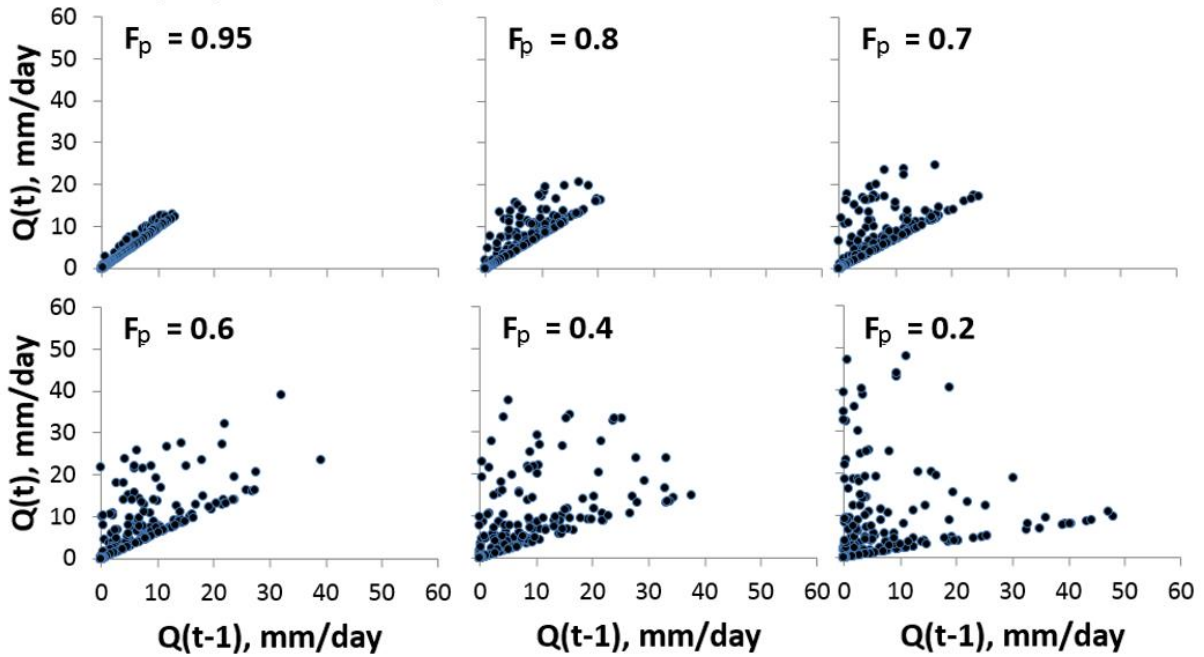
963

964 Figure 4. Effects of the  $F_p$  parameter on hydrographs of daily river flow generated by a random  
965 rainfall generator, with persistent and additional flow components indicated, for two settings  
966 with total rainfall of approximately 1600 and 600 mm/yr (NB river flow is here expressed as mm  
967  $d^{-1}$  rather than as  $m^3 s^{-1}$  as in figure 3)

968

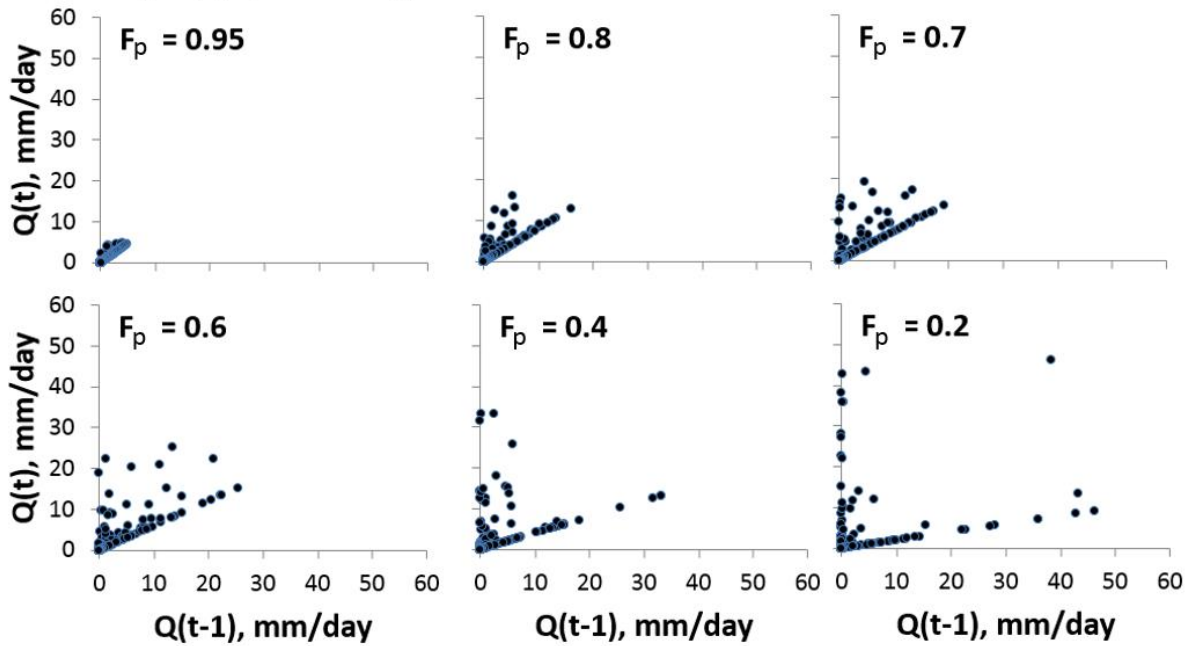
969

**A.** 120 rainy days,  $Q \sim 1600$  mm/yr



970

**B.** 45 rainy days,  $Q \sim 600$  mm/yr

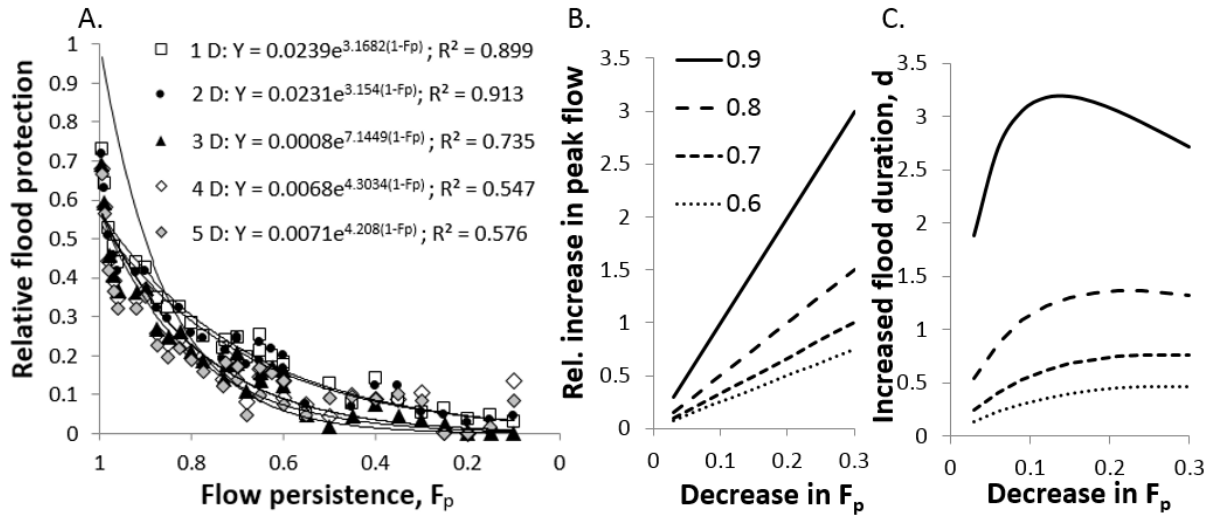


971

972 Figure 5A and B. Temporal autocorrelation of river flow for the same simulations as Figure 4; the  
973 lower envelope of the points indicated slope  $F_p$ , the points above this line the effect of fresh  
974 additions to river flow

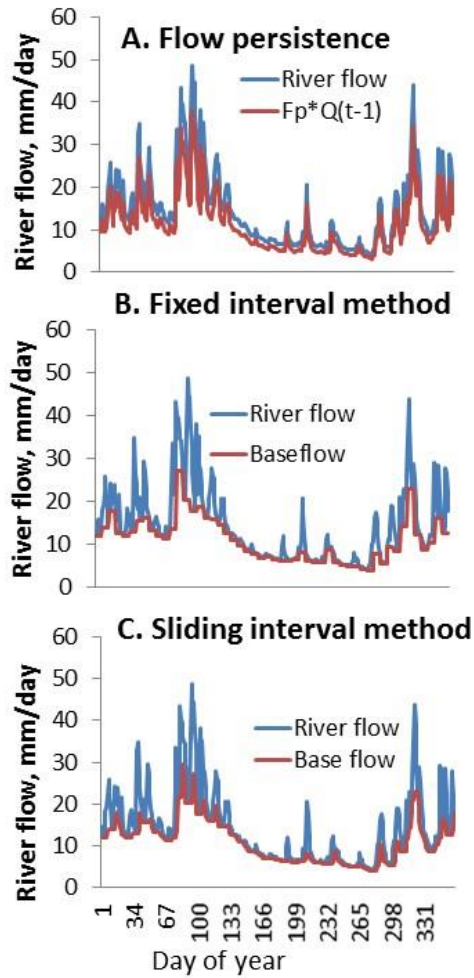
975

976

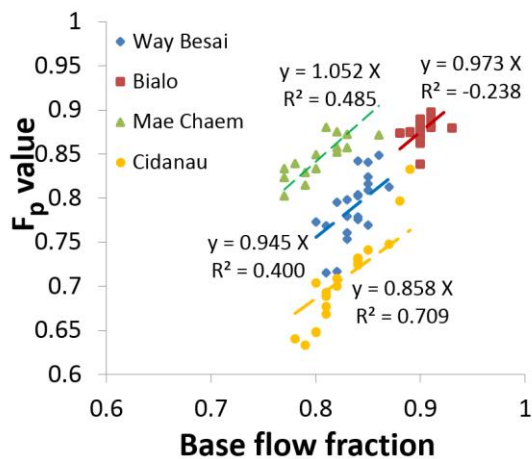


978  
979

980 Figure 6. A. Effects of flow persistence on the relative flood protection (decrease in  
 981 maximum flow measured over a 1 – 5 d period relative to a case with  $F_p = 0$  (a few small  
 982 negative points were replaced by small positive values to allow the exponential fit); B and  
 983 C. effects of a decrease in flow persistence on the volume of water involved in peak flows  
 984 (B; relative to the volume at  $F_p$  is 0.6 – 0.9) and in the duration (in d) of floods (C)  
 985

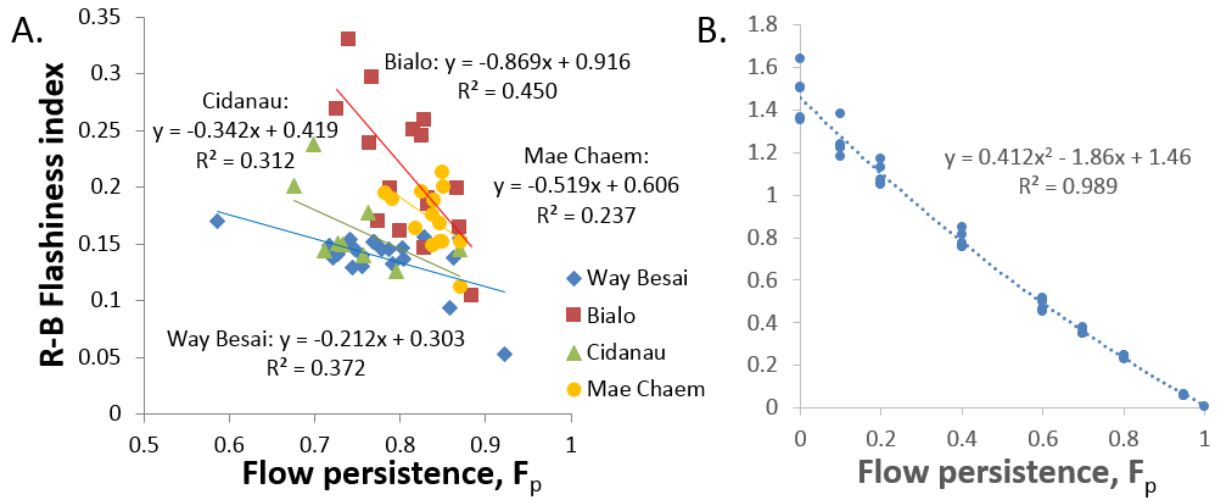


986  
 987 Figure 7. Comparison of base flow separation of a hydrograph according to the flow  
 988 persistence method (A) and two common flow separation methods, respectively with  
 989 fixed (B) and sliding intervals (C)  
 990



991  
 992  
 993 Figure 8. Comparison of yearly data for four Southeast Asian watersheds analysed with  
 994 common flow separation methods (average of results in Fig. 7) and the flow persistence  
 995 method

996  
997



998  
999  
1000  
1001  
1002

Figure 9. Comparison of the Richards-Baker Flashiness Index (Baker et al., 2004) and the flow persistence metric  $F_p$  for A) four Southeast Asian watersheds, B) a series of hydrographs as in Fig. 4A, with 5 replicates per  $F_p$  value

1003 Table 1. Comparison of properties of the Flashiness Index and Flow persistence  $F_p$

Flashiness Index (Baker et al. 2004)	Flow persistence (as defined here)
1. Has direct appeal to non-technical audiences	Potentially similar
2. Where reservoir management rules imply major changes in $\Delta S$ , flashiness still describes implications for flow regimes	Is focused on the effects of changes in (upper) catchment land cover, not where reservoir management determines flow
3. Values depend on the scale of evaluating river flow; no absolute criteria for what is 'healthy'	Similar
4. Increase generally not desirable	Decrease generally not desirable
5. Varies in range [0-2], may need normalizing by division by 2	Varies in range [0-1]
6. Requires full year flow record to be calculated	Can be estimated from any set of sequential flow observations
7. Empirical metric, no direct link to underlying process understanding	Overall $F_p$ can be understood as weighted average of the $F_p$ 's of contributing flow pathways (overland, subsurface and groundwater-based)
8. No directly visible relationship between peak and low flow characteristics	The $F_p$ term low flows and the $(1 - F_p)$ term for peak flows show the water balance logic of a link between peak and low flows
9. Aggregates changes in flow regime; no directly visible link between the performance metric, rainfall (or snow melt) and (vegetation dependent) evapotranspiration	The main water balance terms are directly reflected in the flow descriptions based on $F_p$
10. Substantial empirical data bases available for comparison and meta studies	Not yet

1005 Flood risk reduction and flow buffering as ecosystem  
1006 services: II. Land use and rainfall intensity effects in  
1007 Southeast Asia

1008 Meine van Noordwijk<sup>1,2</sup>, Lisa Tanika<sup>1</sup>, Betha Lusiana<sup>1</sup>

1009 [1]{World Agroforestry Centre (ICRAF), SE Asia program, Bogor, Indonesia}

1010 [2]{Wageningen University, Plant Production Systems, Wageningen, the Netherlands}

1011 Correspondence to: Meine van Noordwijk ([m.vannoordwijk@cgiar.org](mailto:m.vannoordwijk@cgiar.org))

1012 **Abstract**

1013 Watersheds buffer the temporal pattern of river flow relative to the temporal pattern of  
1014 rainfall. This ‘ecosystem service’ is inherent to geology and climate, but buffering also  
1015 responds to human use and misuse of the landscape. Buffering can be part of management  
1016 feedback loops if salient, credible and legitimate indicators are used. The flow persistence  
1017 parameter  $F_p$  in a parsimonious recursive model of river flow (Part I) couples the  
1018 transmission of extreme rainfall events ( $1 - F_p$ ), to the annual base flow fraction of a  
1019 watershed ( $F_p$ ). Here we compare  $F_p$  estimates from four meso-scale watersheds in  
1020 Indonesia (Cidanau, Way Besai, and Bialo) and Thailand (Mae Chaem), with varying climate,  
1021 geology and land cover history, at a decadal time scale. The likely response in each of these  
1022 four to variation in rainfall properties (incl. the maximum hourly rainfall intensity) and land  
1023 cover (comparing scenarios with either more or less forest and tree cover than the current  
1024 situation) was explored through a basic daily water balance model, GenRiver. This model  
1025 was calibrated for each site on existing data, before being used for alternative land cover  
1026 and rainfall parameter settings. In both data and model runs, the wet-season (3-monthly)  $F_p$   
1027 values were consistently lower than dry-season values for all four sites. Across the four  
1028 catchments  $F_p$  values decreased with increasing annual rainfall, but specific aspects of  
1029 watersheds, such as the riparian swamp (peat soils) in Cidanau reduced effects of land use  
1030 change in the upper watershed. Increasing the mean rainfall intensity (at constant monthly  
1031 totals for rainfall) around the values considered typical for each landscape was predicted to  
1032 cause a decrease in  $F_p$  values by between 0.047 (Bialo) and 0.261 (Mae Chaem). Sensitivity of  
1033  $F_p$  to changes in land use change plus changes in rainfall intensity depends on other  
1034 characteristics of the watersheds, and generalizations made on the basis of one or two case  
1035 studies may not hold, even within the same climatic zone. A wet-season  $F_p$  value above 0.7  
1036 was achievable in forest-Agroforestry mosaic case studies. Interannual variability in  $F_p$  is  
1037 large relative to effects of land cover change. Multiple (5-10) years of paired-plot data would  
1038 generally be needed to reject no-change null-hypotheses on the effects of land use change  
1039 (degradation and restoration).  $F_p$  trends over time serve as a holistic scale-dependent  
1040 performance indicator of degrading/recovering watershed health and can be tested for  
1041 acceptability and acceptance in a wider social-ecological context.

1042 **Introduction**

1043 Inherent properties (geology, geomorphology) interact with climate and human modification of  
1044 vegetation, soils, drainage and riparian wetlands in effectuating the degree of buffering that  
1045 watersheds provide (Andréassian 2004; Bruijnzeel, 2004). Buffering of river flow relative to the  
1046 space-time dynamics of rainfall is an ecosystem service, reducing the exposure of people living on  
1047 geomorphological floodplains to high-flow events, and increasing predictability and river flow in dry  
1048 periods (Joshi et al., 2004; Leimona et al., 2015; Part I). In the absence of any vegetation and with a  
1049 sealed surface, river flow will directly respond to the spatial distribution of rainfall, with only the  
1050 travel time to any point of specific interest influencing the temporal pattern of river flow. Any  
1051 persistence or predictability of river flow in such a situation will reflect temporal autocorrelation of  
1052 rainfall, beyond statistical predictability in seasonal rainfall patterns. On the other side of the  
1053 spectrum, river flow can be constant every day, beyond the theoretical condition of constant rainfall,  
1054 in a watershed that provides perfect buffering, by passing all water through groundwater pools that  
1055 have sufficient storage capacity at any time during the year. Both infiltration-limited (Hortonian) and  
1056 saturation-induced use of more rapid flow pathways (inter and overland flows) will reduce the flow  
1057 persistence and make it, at least in part, dependent on rainfall events. Separating the effects of land  
1058 cover (land use), engineering and rainfall on the actual flow patterns of rivers remains a considerable  
1059 challenge (Ma et al., 2014; Verbist et al., 2019). It requires data, models and concepts that can serve  
1060 as effective boundary object in communication with stakeholders (Leimona et al. 2015; van  
1061 Noordwijk et al. 2012, 2016). There is a long tradition in using forest cover as such a boundary  
1062 object, but there is only a small amount of evidence supporting this (Tan-Soo et al., 2014; van Dijk et  
1063 al., 2009; van Noordwijk et al. 2015a; part I).

1064 In part I, we introduced a flow persistence parameter ( $F_p$ ) that links the two, asymmetrical aspects of  
1065 flow dynamics: translating rainfall excess into river flow, and gradually releasing water stored in the  
1066 landscape. The direct link between these two aspects can be seen from equation [4] in part I:

$$1067 \quad Q_t = F_p Q_{t-1} + (1-F_p)(P_t - E_{tx})$$

1068 Where  $Q_t$  and  $Q_{t-1}$  represent river flow on subsequent days,  $P_{tx}$  the precipitation on day  $t$  (or  
1069 preceding precipitation released as snowmelt on day  $t$ ) and  $E_{tx}$  the preceding evapotranspiration  
1070 since the previous precipitation event, creating storage space in the soils of the watershed. The first  
1071 term on the right-hand side of the equation represents the gradual release of stored water, causing  
1072 a slow decline of flow as the pools feeding this flow are gradually depleted. The second term reflects  
1073 the part of fresh additions of water are partitioned over immediate river flow and the increase of  
1074 stocks from which water can be gradually released. The derivation of the link depended on the long  
1075 term water balance, and thus assumed that all out- and inflows are accounted for in the watershed.

1076 Commonly used rainfall-runoff models (including the curve number approach and SWAT models)  
1077 only focus on the second term of the above equation (Ponce et al., 1996; Gassman et al., 2007),  
1078 without link to the first. Various empirical methods for deriving 'base flow' are in use, but details of  
1079 the calculation procedure matter. Results in part I for a number of contrasting meso-scale  
1080 watersheds in Southeast Asia suggested that interannual variation in  $F_p$  within a given watershed  
1081 correlates with both the R-B Flashiness Index (Baker et al., 2004) and the base-flow fraction of  
1082 annual river flow. However, the slope of these relationships varied between watersheds. Here, in  
1083 part II we will further analyse the  $F_p$  results for these watersheds that were selected to represent  
1084 variation in rainfall and land cover, and test the internal consistency of results based on historical

1085 data: two located in the humid and one in the subhumid tropics of Indonesia, and one in the  
1086 unimodal subhumid tropics of northern Thailand.

1087 After exploring the patterns of variation in  $F_p$  estimates derived from actual river flow records, we  
1088 will quantify the sensitivity of the  $F_p$  metric to variations in rainfall intensity and its response, on a  
1089 longer timescale to land cover change. To do so, we will use a model that uses basic water balance  
1090 concepts: rainfall interception, infiltration, water use by vegetation, overland flow, interflow and  
1091 groundwater release, to a spatially structured watershed where travel time from sub watersheds to  
1092 any point of interest modifies the predicted river flow. In the specific model used land cover effects  
1093 on soil conditions, interception and seasonal water use have been included. After testing whether  $F_p$   
1094 values derived from model outputs match those based on empirical data where these exist, we rely  
1095 on the basic logic of the model to make inference on the relative importance of modifying rainfall  
1096 and land cover inputs. With the resulting temporal variation in calculated  $F_p$  values, we consider the  
1097 time frame at which observed shifts in  $F_p$  can be attributed to factors other than chance (that means:  
1098 null-hypotheses of random effects can be rejected with accepted chance of Type I errors).

## 1099 **2. Methods**

### 1100 **2.1 GenRiver model for effects of land cover on river flow**

1101 The GenRiver model (van Noordwijk et al., 2011) is based on a simple water balance concept with a  
1102 daily time step and a flexible spatial subdivision of a watershed that influences the routing of water  
1103 and employs spatially explicit rainfall. At patch level, vegetation influences interception, retention  
1104 for subsequent evaporation and delayed transfer to the soil surface, as well as the seasonal demand  
1105 for water. Vegetation (land cover) also influences soil porosity and infiltration, modifying the  
1106 inherent soil properties. Water in the root zone is modelled separately for each land cover within a  
1107 subcatchment, the groundwater stock is modelled at subcatchment level. The spatial structure of a  
1108 watershed and the routing of surface flows influences the time delays to any specified point of  
1109 interest, which normally includes the outflow of the catchment. Land cover change scenarios are  
1110 interpolated annually between time-series (measured or modelled) data. The model may use  
1111 measured rainfall data, or use a rainfall generator that involves Markov chain temporal  
1112 autocorrelation (rain persistence). As our data sources are mostly restricted to daily rainfall  
1113 measurements and the infiltration model compares instantaneous rainfall to infiltration capacity, a  
1114 stochastic rainfall intensity was applied at subcatchment level, driven by the mean as parameter and  
1115 a standard deviation for a normal distribution (truncated at 3 standard deviations from the mean)  
1116 proportional to it via a coefficient of variation as parameter. For the Mae Chaem site in N Thailand  
1117 data by Dairaku et al. (2004) suggested a mean of less than 3 mm/hr. For the three sites in Indonesia  
1118 we used 30 mm/hr, based on Kusumastuti et al. (2016). Appendix 1 provides further detail on the  
1119 GenRiver model. The model itself, a manual and application case studies are freely available  
1120 (<http://www.worldagroforestry.org/output/genriver-genetic-river-model-river-flow>;van Noordwijk  
1121 et al., 2011).

### 1122 **2.2 Empirical data-sets, model calibration**

1123 Table 1 and Figure 1 provide summary characteristics and the location of river flow data used in four  
1124 meso-scale watersheds for testing the  $F_p$  algorithm and application of the GenRiver model. Figure 1  
1125 includes a water tower category in the agro-ecological zones; this is defined on the basis of a ratio of

1126 precipitation and potential evapotranspiration of more than 0.65, and a product of that ratio and  
1127 relative elevation exceeding 0.277.

1128       ⇒ Table 1

1129       ⇒ Figure 1

1130 As major parameters for the GenRiver model were not independently measured for the respective  
1131 watersheds, we tuned (calibrated) the model by modifying parameters within a predetermined  
1132 plausible range, and used correspondence with measured hydrograph as test criterion (Kobolt et al.  
1133 2008). We used the Nash-Sutcliffe Efficiency (NSE) parameter (target above 0.5) and bias (less than  
1134 25%) as test criteria and targets. Meeting these performance targets (Moriassi et al., 2007), we  
1135 accepted the adjusted models as basis for describing current conditions and exploring model  
1136 sensitivity. The main site-specific parameter values are listed in Table 2 and (generic) land cover  
1137 specific default parameters in Table 3.

1138       ⇒ Table 2

1139       ⇒ Table 3

1140 Table 4 describes the six scenarios of land use change that were evaluated in terms of their  
1141 hydrological impacts. Further description on the associated land cover distribution for each scenario  
1142 in the four different watersheds is depicted in Appendix 2.

1143       ⇒ Table 4

## 1144 **2.3 Bootstrapping to estimate the minimum observation**

1145 The bootstrap methods (Efron and Tibshirani, 1986) is a resampling methods that is commonly used  
1146 to generate ‘surrogate population’ for the purpose of approximating the sampling distribution of a  
1147 statistic. In this study, the bootstrap approach was used to estimate the minimum number of  
1148 observation (or yearly data) required for a pair-wise comparison test between two time-series of  
1149 stream flow or discharge data (representing two scenarios of land use distributions) to be  
1150 distinguishable from a null-hypothesis of no effect. The pair-wise comparison test used was  
1151 Kolmogorov-Smirnov test that is commonly used to test the distribution of discharge data (Zhang et al.  
1152 al, 2006). We built a simple macro in R (R Core Team, 2015) that entails the following steps:

1153       (i) Bootstrap or resample with replacement 1000 times from both time-series discharge data  
1154           with sample size  $n$ ;

1155       (ii) Apply the Kolmogorov-Smirnov test to each of the 1000 generated pair-wise discharge data,  
1156           and record the P-value;

1157       (iii) Perform (i) and (ii) for different size of  $n$ , ranging from 5 to 50.

1158       (iv) Tabulate the p-value from the different sample size  $n$ , and determine the value of  $n$  when the  
1159           p-value reached equal to or less than 0.025 (or equal to the significance level of 5%). The  
1160           associated  $n$  represents the minimum number of observations required.

1161 Appendix 3 provides an example of the macro in R used for this analysis.

## 1162 **3. Results**

### 1163 **3.1 Empirical data of flow persistence as basis for model parameterization**

1164 Inter-annual variability of  $F_p$  estimates derived for the four catchments (Figure 2) was of the order of  
1165 0.1 units, while the intra-annual variability between dry and rainy seasons was 0.1-0.2. For all years  
1166 and locations, rainy season  $F_p$  values, with mixed flow pathways, were consistently below dry-season  
1167 values, dominated by groundwater flows. If we can expect  $F_{p,i}$  and  $F_{p,o}$  (see equation 8 in part I) to be  
1168 approximately 0.5 and 0, this difference between wet and dry periods implies a 40% contribution of  
1169 interflow in the wet season, a 20% contribution of overland flow or any combination of the two  
1170 effects.

1171 Overall the estimates from modelled and observed data are related with 16% deviating more than  
1172 0.1 and 3% more than 0.15 (Figure 3). As the Moriasi et al. (2007) performance criteria for the  
1173 hydrographs were met by the calibrated models for each site, we tentatively accept the model to be  
1174 a basis for sensitivity study of  $F_p$  to modifications to land cover and/or rainfall

1175       ⇒ Figure 2

1176       ⇒ Figure 3

### 1177 **3.2 Comparing $F_p$ effects of rainfall intensity and land cover change**

1178 A direct comparison of model sensitivity to changes in mean rainfall intensity and land use change  
1179 scenarios is provided in Figure 4. Varying the mean rainfall intensity over a factor 7 shifted the  $F_p$   
1180 value by only 0.047 and 0.059 in the case of Bialo and Cidanau, respectively, but by 0.128 in Way  
1181 Besai and 0.261 in Mae Chaem (Figure 4A). The impact of the land use change scenarios on  $F_p$  was  
1182 smallest in Cidanau (0.026), intermediate in Way Besai (0.048) and relatively large in Bialo and Mae  
1183 Chaem, at 0.080 and 0.084, respectively (Figure 4B). The order of  $F_p$  across the land use change  
1184 scenarios was mostly consistent between the watersheds, but the contrast between the  
1185 Reforestation and Natural Forest scenario was largest in Mae Chaem and smallest in Way Besai. In  
1186 Cidanau, Way Besai and Mae Chaem, variations in rainfall were 2.2 to 3.1 times more effective than  
1187 land use change in shifting  $F_p$ , in Bialo its relative effect was only 58%. Apparently, the sensitivity to  
1188 changes in land use change plus changes in rainfall intensity depends on other characteristics of the  
1189 watersheds, and generalizations made on the basis of one or two case studies may not hold, even  
1190 within the same climatic zone.

1191       ⇒ Figure 4

### 1192 **3.3 Further analysis of $F_p$ effects for scenarios of land cover change**

1193 Among the four watersheds there is consistency in that the 'forest' scenario has the highest, and the  
1194 'degraded lands' the lowest  $F_p$  value (Figure 5), but there are remarkable differences as well: in  
1195 Cidanau the interannual variation in  $F_p$  is clearly larger than land cover effects, while in the Way  
1196 Besai the spread in land use scenarios is larger than interannual variability. In Cidanau a peat swamp  
1197 between most of the catchment and the measuring point buffers most of land cover related  
1198 variation in flow, but not the interannual variability. Considering the frequency distributions of  $F_p$   
1199 values over a 20 year period, we see one watershed (Way Besai) where the forest stands out from all  
1200 others, and one (Bialo) where the degraded lands are separate from the others. Given the degree of  
1201 overlap of the frequency distributions, it is clear that multiple years of empirical observations will be  
1202 needed before a change can be affirmed.

1203 Figure 5 shows the frequency distributions of expected effect sizes on  $F_p$  of a comparison of any land  
1204 cover with either forest or degraded lands. Table 5 translates this information to the number of

1205 years that a paired plot (in the absence of measurement error) would have to be maintained to  
1206 reject a null-hypothesis of no effect, at  $p=0.05$ . As the frequency distributions of  $F_p$  differences of  
1207 paired catchments do not match a normal distribution, a Kolmogorov-Smirnov test can be used to  
1208 assess the probability that a no-difference null hypothesis can yield the difference found. By  
1209 bootstrapping within the years where simulations supported by observed rainfall data exist, we  
1210 found for the Way Besai catchment, for example, that 20 years of data would be needed to assert (at  
1211  $P = 0.05$ ) that the Reforestation scenario differs from Agroforestation, and 16 years that it differs  
1212 from Actual and 11 years that it differs from Degrade. In practice, that means that empirical  
1213 evidence that survives statistical tests will not emerge, even though effects on watershed health are  
1214 real.

1215       ⇒ Figure 5

1216       ⇒ Table 5

1217 At process-level the increase in 'overland flow' in response to soil compaction due to land cover  
1218 change has a clear and statistically significant relationship with decreasing  $F_p$  values in all catchments  
1219 (Figure 6), but both year-to-year variation within a catchment and differences between catchments  
1220 influence the results as well, leading to considerable spread in the biplot. Contrary to expectations,  
1221 the disappearance of 'interflow' by soil compaction is not reflected in measurable change in  $F_p$  value.  
1222 The temporal difference between overland and interflow (one or a few days) gets easily blurred in  
1223 the river response that integrates over multiple streams with variation in delivery times; the  
1224 difference between overland- or interflow and baseflow is much more pronounced. Apparently,  
1225 according to our model, the high macroporosity of forest soils that allows interflow and may be the  
1226 'sponge' effect attributed to forest, delays delivery to rivers by one or a few days, with little effect on  
1227 the flow volumes at locations downstream where flow of multiple days accumulates. The difference  
1228 between overland- or interflow and baseflow in time-to-river of rainfall peaks is much more  
1229 pronounced.

1230       ⇒ Figure 6

1231 Tree cover has two contradicting effects on baseflow: it reduces the surplus of rainfall over  
1232 evapotranspiration (annual water yield) by increased evapotranspiration (especially where  
1233 evergreen trees or trees with a large canopy interception are involved), but it potentially increases  
1234 soil macroporosity that supports infiltration and interflow, with relatively little effect on water  
1235 holding capacity measured as 'field capacity' (after runoff and interflow have removed excess  
1236 water). Figure 7 shows that the total volume of baseflow differs more between sites and their  
1237 rainfall pattern than it varies with tree cover. Between years total evapotranspiration and baseflow  
1238 totals are positively correlated, but for a given rainfall there is a trade-off. Overall these results  
1239 support the conclusion that generic effects of deforestation on decreased flow persistence, and of  
1240 (agro)/(re)-forestation on increased flow persistence are small relative to interannual variability due  
1241 to specific rainfall patterns, and that it will be hard for any empirical data process to pick-up such  
1242 effects, even if they are qualitatively aligned with valid process-based models.

1243       ⇒ Figure 7

#### 1244       **4. Discussion**

1245 In the discussion of Part I the credibility questions on replicability of the  $F_p$  metric and its sensitivity  
1246 to details of rainfall pattern versus land cover as potential causes of variation were seen as requiring

1247 case studies in a range of contexts. Although the four case studies in Southeast Asia presented here  
1248 cannot be claimed to represent the global variation in catchment behaviour (with absence of a  
1249 snowpack and its dynamics as an obvious element of flow buffering not included), the diversity of  
1250 responses among these four already point to challenges for any generic interpretation of the degree  
1251 of flow persistence that can be achieved under natural forest cover, as well as its response to land  
1252 cover change.

1253 The empirical data summarized here for (sub)humid tropical sites in Indonesia and Thailand show  
1254 that values of  $F_p$  above 0.9 are scarce in the case studies provided, but values above 0.8 were found,  
1255 or inferred by the model, for forested landscapes. Agroforestry landscapes generally presented  $F_p$   
1256 values above 0.7, while open-field agriculture or degraded soils led to  $F_p$  values of 0.5 or lower. Due  
1257 to differences in local context, it may not be feasible to relate typical  $F_p$  values to the overall  
1258 condition of a watershed, but temporal change in  $F_p$  can indicate degradation or restoration if a  
1259 location-specific reference can be found. The difference between wet and dry season  $F_p$  can be  
1260 further explored in this context. The dry season  $F_p$  value primarily reflects the underlying geology,  
1261 with potential modification by engineering and operating rules of reservoirs, the wet season  $F_p$  is  
1262 generally lower due to partial shifts to overland and interflow pathways. Where further uncertainty  
1263 is introduced by the use of modelled rather than measured river flow, the lack of fit of models  
1264 similar to the ones we used here would mean that scenario results are indicative of directions of  
1265 change rather than a precision tool for fine-tuning combinations of engineering and land cover  
1266 change as part of integrated watershed management.

1267 The differences in relative response of the watersheds to changes in mean rainfall intensity and land  
1268 cover change, suggest that generalizations derived from one or a few case studies are to be  
1269 interpreted cautiously. If land cover change would influence details of the rainfall generation process  
1270 (arrow 10 in Figure 1 of part I; e.g. through release of ice-nucleating bacteria Morris et al., 2014; van  
1271 Noordwijk et al., 2015b) this can easily dominate over effects via interception, transpiration and soil  
1272 changes.

1273 Our results indicate an intra-annual variability of  $F_p$  values between wet and dry seasons of around  
1274 0.2 in the case studies, while interannual variability in either annual or seasonal  $F_p$  was generally in  
1275 the 0.1 range. The difference between observed and simulated flow data as basis for  $F_p$  calculations  
1276 was mostly less than 0.1. With current methods, it seems that effects of land cover change on flow  
1277 persistence that shift the  $F_p$  value by about 0.1 are the limit of what can be asserted from empirical  
1278 data (with shifts of that order in a single year a warning sign rather than a firmly established change).  
1279 When derived from observed river flow data  $F_p$  is suitable for monitoring change (degradation,  
1280 restoration) and can be a serious candidate for monitoring performance in outcome-based  
1281 ecosystem service management contracts. Choice of the part of the year for which  $F_p$  changes are  
1282 used as indicator may have to depend on the seasonal patterns of rainfall.

1283 In view of our results the lack of robust evidence in the literature of effects of change in forest and  
1284 tree cover on flood occurrence may not be a surprise; effects are subtle and most data sets contain  
1285 considerable variability. Yet, such effects are consistent with current process and scaling knowledge  
1286 of watersheds.

1287 In summarizing findings on the  $F_p$  metric, we can compare it with existing ones across the seven  
1288 questions raised in Fig. 1 of part I. Comparator metrics can derive from various data sources,

1289 including the amount (and/or quality) of forest cover upstream, the fraction of flows that is  
1290 technically controlled, direct records of river flow (over a short or longer time period), records of  
1291 rainfall and/or models that combine landscape properties, climate and land cover. Tentative scoring  
1292 for these metrics (Table 6) suggest that the  $F_p$  metric is an efficient tool for data-scarce  
1293 environments, as it indicates aspects of hydrographs that so far required multi-annual records of  
1294 river flow.

1295 → Table 6

## 1296 **Conclusion**

1297 Overall, our analysis suggests that the level of flow buffering achieved depends on both land cover  
1298 (including its spatial configuration and effects on soil properties) and space-time patterns of rainfall  
1299 (including maximum rainfall intensity as determinant of overland flow). Generalizations on dominant  
1300 influence of either, derived from one or a few case studies are to be interpreted cautiously. If land  
1301 cover change would influence details of the rainfall generation process this can easily dominate over  
1302 effects via interception, transpiration and soil changes. Multi-year data will generally be needed to  
1303 attribute observed changes in flow buffering to degradation/restoration of watersheds, rather than  
1304 specific rainfall events. With current methods, it seems that effects of land cover change on flow  
1305 persistence that shift the  $F_p$  value by about 0.1 are the limit of what can be asserted from empirical  
1306 data, with shifts of that order in a single year a warning sign rather than a firmly established change.  
1307 When derived from observed river flow data  $F_p$  is suitable for monitoring change (degradation,  
1308 restoration) and can be a serious candidate for monitoring performance in outcome-based  
1309 ecosystem service management contracts. Watershed health is here characterized through the flow  
1310 pattern it generates, leaving the attribution to land cover, rainfall pattern and engineering of that  
1311 pattern and of changes in pattern to further location-specific analysis, just as a symptom of a high  
1312 body temperature can indicate health, but not diagnose the specific illness causing it.

1313 The data sets analysed so far did not indicate that the flow persistence at high flows differed from  
1314 that at lower flows within the same season, but in other circumstances this may not be the case and  
1315 further care may be needed to use  $F_p$  values beyond the measurement period in which they were  
1316 derived. While a major strength of the  $F_p$  method over existing procedures for parameterizing curve  
1317 number estimates, for example, is that the latter depend on scarce observations during extreme  
1318 events and  $F_p$  can be estimated for any part of the flow record, the reliability of  $F_p$  estimates will still  
1319 increase with the length of the observation period.

1320 Further tests on the performance of the  $F_p$  metric and its standard incorporation into the output  
1321 modules of river flow and watershed management models will broaden the basis for interpreting the  
1322 value ranges that can be expected for well-functioning watersheds in various conditions of climate,  
1323 topography, soils, vegetation and engineering interventions. Such a broader empirical base could  
1324 test the possible use of  $F_p$  as performance metric for watershed rehabilitation efforts.

## 1325 **Data availability**

1326 Table 7 specifies the rainfall and river flow data we used for the four basins and specifies the links to  
1327 detailed descriptions.

1328 ⇨ Table 7

1329 **Acknowledgements**

1330 This research is part of the Forests, Trees and Agroforestry research program of the CGIAR. Several  
1331 colleagues contributed to the development and early tests of the  $F_p$  method. Thanks are due to  
1332 Thoha Zulkarnain for assistance with Figure 1 and to Eike Luedeling, Sonya Dewi, Sampurno  
1333 Bruijnzeel and two anonymous reviewers for comments on an earlier version of the manuscript.

1334 **References**

- 1335 Andréassian, V.: Waters and forests: from historical controversy to scientific debate, *Journal of*  
1336 *Hydrology*, 291, 1–27, 2004.
- 1337 Baker, D.B., Richards, R.P., Loftus, T.T. and Kramer, J.W.: A new flashiness index: Characteristics and  
1338 applications to midwestern rivers and streams. *Journal of the American Water Resources*  
1339 *Association*, Paper No. 03095, 2004.
- 1340 Bruijnzeel, L.A.: Hydrological functions of tropical forests: not seeing the soil for the trees, *Agr.*  
1341 *Ecosyst. Environ.*, 104, 185–228, 2004.
- 1342 Dairaku K., Emori, S., and Taikan, T.: Rainfall Amount, Intensity, Duration, and Frequency  
1343 Relationships in the Mae Chaem Watershed in Southeast Asia, *Journal of Hydrometeorology*, 5,  
1344 458-470, 2004.
- 1345 Efron, B and Tibshirani, R.: Bootstrap Methods for Standard Errors, Confidence Intervals, and Other  
1346 Measures of Statistical Accuracy. *Statistical Science* 1 (1): 54-75, 1986.
- 1347 Gassman, P.W., Reyes, M.R., Green, C.H. and Arnold, J.G.: The soil and water assessment tool: historical  
1348 development, applications, and future research directions. *Transactions of the ASABE*, 50(4), 1211-1250,  
1349 2007.
- 1350 Joshi, L., Schalenbourg, W., Johansson, L., Khasanah, N., Stefanus, E., Fagerström, M.H., and van  
1351 Noordwijk, M.: Soil and water movement: combining local ecological knowledge with that of  
1352 modellers when scaling up from plot to landscape level, In: van Noordwijk, M., Cadisch, G. and  
1353 Ong, C.K. (Eds.) *Belowground Interactions in Tropical Agroecosystems*, CAB International,  
1354 Wallingford (UK), 349-364, 2004.
- 1355 Kobold, M., Suselj, K., Polajnar, J., and Pogacnik, N.: Calibration Techniques Used For HBV  
1356 Hydrological Model In Savinja Catchment, In: XXIVth Conference of the Danubian Countries On  
1357 The Hydrological Forecasting And Hydrological Bases Of Water Management, 2008.
- 1358 Kusumastuti, D.I., Jokowinarno, D., van Rafi'i, C.H., and Yuniarti, F.: Analysis of rainfall characteristics  
1359 for flood estimation in Way Awi watershed, *Civil Engineering Dimension*, 18, 31-37, 2016
- 1360 Leimona, B., Lusiana, B., van Noordwijk, M., Mulyoutami, E., Ekadinata, A., and Amaruzama, S.:  
1361 Boundary work: knowledge co-production for negotiating payment for watershed services in  
1362 Indonesia, *Ecosystems Services*, 15, 45–62, 2015.
- 1363 Ma, X., Lu, X., van Noordwijk, M., Li, J.T., and Xu, J.C.: Attribution of climate change, vegetation  
1364 restoration, and engineering measures to the reduction of suspended sediment in the Kejie  
1365 catchment, southwest China, *Hydrol. Earth Syst. Sci.*, 18, 1979–1994, 2014.

1366 Moriasi, D.N., Arnold, J.G., Van Liew, M.W., Bingner, R.L., Harmel, R.D., and Veith, T.L.: Model  
1367 Evaluation Guidelines For Systematic Quantification Of Accuracy In Watershed Simulations,  
1368 American Society of Agricultural and Biological Engineers, 20(3),885-900, 2001

1369 Morris, C.E., Conen, F., Huffman, A., Phillips, V., Pöschl, U., and Sands, D.C.: Bioprecipitation: a  
1370 feedback cycle linking Earth history, ecosystem dynamics and land use through biological ice  
1371 nucleators in the atmosphere, *Glob Change Biol*, 20, 341-351. 2014.

1372 Ponce, V.M. and Hawkins, R.H.: Runoff curve number: Has it reached maturity? *Journal of Hydrologic*  
1373 *Engineering*, 1(1), 11-19, 1996

1374 R Core Team R: A language and environment for statistical computing. R Foundation for Statistical  
1375 Computing, Vienna, Austria, URL <http://www.R-project.org/>, 2015

1376 Tan-Soo, J.S., Adnan, N., Ahmad, I., Pattanayak, S.K., and Vincent, J.R.: Econometric Evidence on  
1377 Forest Ecosystem Services: Deforestation and Flooding in Malaysia. *Environmental and Resource*  
1378 *Economics*, on-line: <http://link.springer.com/article/10.1007/s10640-014-9834-4>, 2014.

1379 van Dijk, A.I., van Noordwijk, M., Calder, I.R., Bruijnzeel, L.A., Schellekens, J., and Chappell, N.A.:  
1380 Forest-flood relation still tenuous – comment on ‘Global evidence that deforestation amplifies  
1381 flood risk and severity in the developing world’, *Global Change Biology*, 15, 110-115, 2009.

1382 van Noordwijk, M., Widodo, R.H., Farida, A., Suyamto, D., Lusiana, B., Tanika, L., and Khasanah, N.:  
1383 GenRiver and FlowPer: Generic River and Flow Persistence Models. User Manual Version 2.0,  
1384 Bogor, Indonesia, World Agroforestry Centre (ICRAF) Southeast Asia Regional Program, 2011.

1385 van Noordwijk, M., Leimona, B., Jindal, R., Villamor, G.B., Vardhan, M., Namirembe, S., Catacutan, D.,  
1386 Kerr, J., Minang, P.A., and Tomich, T.P.: Payments for Environmental Services: evolution towards  
1387 efficient and fair incentives for multifunctional landscapes, *Annu. Rev. Environ. Resour.*, 37, 389-  
1388 420, 2012.

1389 van Noordwijk, M., Leimona, B., Xing, M., Tanika, L., Namirembe, S., and Suprayogo, D.: Water-  
1390 focused landscape management. *Climate-Smart Landscapes: Multifunctionality In Practice*, eds  
1391 Minang PA et al.. Nairobi, Kenya: World Agroforestry Centre (ICRAF), 179-192, 2015a.

1392 van Noordwijk, M., Bruijnzeel, S., Ellison, D., Sheil, D., Morris, C., Gutierrez, V., Cohen, J., Sullivan, C.,  
1393 Verbist, B., and Muys, B.: Ecological rainfall infrastructure: investment in trees for sustainable  
1394 development, ASB Brief no 47, Nairobi, ASB Partnership for the Tropical Forest Margins, 2015b.

1395 van Noordwijk, M., Kim, Y-S., Leimona, B., Hairiah, K., Fisher, L.A.: Metrics of water security,  
1396 adaptive capacity and Agroforestry in Indonesia. *Current Opinion on Environmental Sustainability*  
1397 (in press: <http://dx.doi.org/10.1016/j.cosust.2016.10.004>). 2016

1398 Verbist, B., Poesen, J., van Noordwijk, M. Widiyanto, Suprayogo, D., Agus, F., and Deckers, J.: Factors  
1399 affecting soil loss at plot scale and sediment yield at catchment scale in a tropical volcanic  
1400 Agroforestry landscape, *Catena*, 80, 34-46, 2010.

1401 Zhang, Q., Liu, C., Xu, C., Xu, and Jiang T.: Observed trends of annual maximum water level and  
1402 streamflow during past 130 years in the Yangtze River basin, China, *Journal of Hydrology*, 324,  
1403 255-265, 2006.

1404

1405 Table 1. Basic physiographic characteristics of the four study watersheds

Parameter	Bialo	Cidanau	Mae Chaem	Way Besai
Location	South Sulawesi, Indonesia	West Java, Indonesia	Northern Thailand	Lampung, Sumatera, Indonesia
Coordinates	5.43 S, 120.01 E	6.21 S, 105.97 E	18.57 N, 98.35 E	5.01 S, 104.43 E
Area (km <sup>2</sup> )	111.7	241.6	3892	414.4
Elevation (m a.s.l.)	0 – 2874	30 – 1778	475-2560	720-1831
Flow pattern	Parallel	Parallel (with two main river flow that meet in the downstream area)	Parallel	Radial
Land cover type	Forest (13%) Agroforest (59%) Crops (22%) Others (6%)	Forest (20%) Agroforest (32%) Crops (33%) Others (11%) Swamp(4%)	Forest (evergreen, deciduous and pine) (84%) Crops (15%) Others (1%)	Forest (18%) Coffee (monoculture and multistrata) (64%) Crop and Horticulture (12%) Others (6%)
Mean annual rainfall, mm	1695	2573	1027	2474
Wet season	April – June	January - March	July - September	January - March
Dry season	July - September	July - September	January - March	July - September
Mean annual runoff, mm	947	917	259	1673
Major soils	Inceptisols	Inceptisols	Ultisols, Entisols	Andisols

1406

1407 Table 2. Parameters of the GenRiver model used for the four site specific simulations (van Noordwijk  
1408 et al., 2011 for definitions of terms; sequence of parameters follows the pathway of water)

Parameter	Definition	Unit	Bialo	Cidanau	Mae Chaem	Way Besai
RainIntensMean	Average rainfall intensity	mm hr <sup>-1</sup>	30	30	3	30
RainIntensCoefVar	Coefficient of variation of rainfall intensity	mm hr <sup>-1</sup>	0.8	0.3	0.5	0.3

RainInterceptDripRt	Maximum drip rate of intercepted rain	mm hr <sup>-1</sup>	80	10	10	10
RainMaxIntDripDur	Maximum dripping duration of intercepted rain	hr	0.8	0.5	0.5	0.5
InterceptEffectontrans	Rain interception effect on transpiration	-	0.35	0.8	0.3	0.8
MaxInfRate	Maximum infiltration capacity	mm d <sup>-1</sup>	580	800	150	720
MaxInfSubsoil	Maximum infiltration capacity of the sub soil	mm d <sup>-1</sup>	80	120	150	120
PerFracMultiplier	Daily soil water drainage as fraction of groundwater release fraction	-	0.35	0.13	0.1	0.1
MaxDynGrWatStore	Dynamic groundwater storage capacity	mm	100	100	300	300
GWReleaseFracVar	Groundwater release fraction, applied to all subcatchments	-	0.15	0.03	0.05	0.1
Tortuosity	Stream shape factor	-	0.4	0.4	0.6	0.45
Dispersal Factor	Drainage density	-	0.3	0.4	0.3	0.45
River Velocity	River flow velocity	m s <sup>-1</sup>	0.4	0.7	0.35	0.5

1410 Table 3. GenRiver defaults for land use specific parameter values, used for all four watersheds  
 1411 (BD/BDref indicates the bulk density relative to that for an agricultural soil pedotransfer function;  
 1412 see van Noordwijk et al., 2011)

Land cover Type	Potential interception (mm/d)	Relative drought threshold	BD/BDref
Forest <sup>1</sup>	3.0 - 4.0	0.4 - 0.5	0.8 - 1.1
Agroforestry <sup>2</sup>	2.0 - 3.0	0.5 - 0.6	0.95 - 1.05
Monoculture tree <sup>3</sup>	1.0	0.55	1.08
Annual crops	1.0 - 3.0	0.6 - 0.7	1.1 - 1.5
Horticulture	1.0	0.7	1.07
Rice field <sup>4</sup>	1.0 - 3.0	0.9	1.1 - 1.2
Settlement	0.05	0.01	1.3
Shrub and grass	2.0 - 3.0	0.6	1.0 - 1.07
Cleared land	1.0 - 1.5	0.3 - 0.4	1.1 - 1.2

1413 Note: 1. Forest: primary forest, secondary forest, swamp forest, evergreen forest, deciduous forest

1414 2. Agroforestry: mixed garden, coffee, cocoa, clove

1415 3. Monoculture : coffee

1416 4. Rice field: irrigation and rainfed

1417

1418 Table 4. Land use scenarios explored for four watersheds

Scenario	Description
Natural Forest	Full natural forest, hypothetical reference scenario
Reforestation	Reforestation, replanting shrub, cleared land, grass land and some agricultural area with forest
Agroforestation	Agroforestry scenario, maintaining Agroforestry areas and converting shrub, cleared land, grass land and some of agricultural area into Agroforestry
Actual	Baseline scenario, based on the actual condition of land cover change during the modelled time period
Agriculture	Agriculture scenario, converting some of tree based plantations, cleared land, shrub and grass land into rice fields or dry land agriculture, while maintain existing forest
Degrading	No change in already degraded areas, while converting most of forest and Agroforestry area into rice fields and dry land agriculture

1419

1420

1421 Table 5. Number of years of observations required to estimate flow persistence to reject the null-  
 1422 hypothesis of 'no land use effect', at p-value = 0.05 using Kolmogorov-Smirnov test. The probability  
 1423 of the test statistic in the first significant number is provided between brackets and where the  
 1424 number of observations exceeds the time series available, results are given in *italics*

A. Natural Forest as reference				
	Refores- tation	Agrofo- restation	Actual	Agricultural
<b>Way Besai (N=32)</b>				
Reforestation		20 (0.035)	16 (0.037)	13 (0.046)
Agroforestation			n.s.	n.s.
Actual				n.s.
Agricultural				
Degrading				
<b>Bialo (N=18)</b>				
Reforestation		n.s.	n.s.	37 (0.04)
Agroforestation			n.s.	n.s.
Actual				n.s.
Agricultural				
Degrading				
<b>Cidanau (N=20)</b>				
Reforestation		n.s.	n.s.	32 (0.037)
Agroforestation			n.s.	n.s.
Actual				n.s.
Agricultural				
Degrading				
<b>Mae Chaem (N=15)</b>				
Reforestation		n.s.	23 (0.049)	18 (0.050)
Agroforestation			45 (0.037)	33 (0.041)

Actual		33 (0.041)
Agricultural		

**B. Degrading scenario as reference**

<b>Way Besai (N=32)</b>	Natural forest	Reforestation	Agroforestation	Actual	Agriculture
Natural forest		n.s.	17 (0.042)	13 (0.046)	7 (0.023)
Reforestation			21 (0.037)	19 (0.026)	7 (0.023)
Agroforestation				n.s.	28 (0.046)
Actual					30 (0.029)
Agriculture					

<b>Bialo (N=18)</b>	Natural forest	Reforestation	Agroforestation	Actual	Agriculture
Natural forest		n.s.	n.s.	41 (0.047)	19 (0.026)
Reforestation			n.s.	n.s.	32 (0.037)
Agroforestation				n.s.	n.s.
Actual					n.s.
Agriculture					

<b>Cidanau (N=20)</b>	Natural forest	Reforestation	Agroforestation	Actual	Agriculture
Natural forest		n.s.	n.s.	33 (0.041)	8 (0.034)
Reforestation			n.s.	n.s.	15 (0.028)
Agroforestation				n.s.	n.s.
Actual					25 (0.031)
Agriculture					

<b>Mae Chaem (N=15)</b>	Natural forest	Reforestation	Actual	Agriculture
Natural forest		n.s.	25 (0.031)	12 (0.037)
Reforestation			n.s.	18 (0.050)

Agroforestation

18 (0.050)

Actual

1425

---

1426 Table 6. Comparison of metrics at various points in the causal network (Fig. 2 of Paper I) that can  
 1427 support watershed management and prevention of flood damage on the list of seven issues (I – VII)  
 1428 introduced in Fig. 1 Paper I\*.

	Terrain-based (7A and 5 in Fig. 2 of part I)		Based on river flow characteristics (4 in Fig. 2 of part I)						Integrated (5-7) terrain + climate + land use + river flow models	
Issues*	Forest cover	Fraction of flow technically regulated	$Q_{max} / Q_{min}$	Flashiness index	Flow frequency analysis	Curve-number (rainfall-runoff)	Base-flow	Flow persistence, $F_p$	Spatial analysis	Spatial water flow model
Range	0-100%	0-100%	1 - $\omega$	0 - 2		1 - 100	0-100%	0 - 1		
IA	No	Yes	No	Yes	Yes	Yes	No	Yes	Partially	Yes
IB	No	Yes	No	No	Yes	No	Yes	Yes	Partially	Yes
IIA	Not	Partially	Not	Not	Yes	Partially	Partially	Partially	Partially	Partially
IIB	Partially	Yes	Not	Not	Not	Partially	Partially	Partially	Partially	Yes
IIC	Not	Partially	Not	Partially	Partially	Not	Partially	Partially	Partially	Yes
III	Partially	Partially	Not	Partially	Yes	Partially	Partially	Partially	Partially	Yes
IVA	Single	-	Single	Single	Multi	Multi	Single	Single	Single	Single
IVB	Robust	Robust	Sensitive	Sensitive	Sensitive	Sensitive	Robust	Robust	Robust	Robust
V	Partially	Not	Not	Yes	No	No	Partially	Yes	Partially	Partially
VI	Not	Not	Not	Partially	Not	Not	Not	Yes	Partially	Partially
VII	Not	Neutral	Not	Yes	Yes	Neutral	Neutral	Yes	Yes	Yes

- 1429 I. Does the indicator relate to important aspects of watershed behaviour (A. Flood damage  
 1430 prevention; B. Low flow water availability)?
- 1431 II. Does its quantification help to select management actions? (A. Risk assessment, insurance  
 1432 design; B. Spatial planning, engineering interventions; C. Fine-tuning land use)
- 1433 III. Is it consistent with current understanding of key processes
- 1434 IV. Are data requirements feasible (A. Lowest temporal resolution for estimates (years); B.  
 1435 Consistency of numerical results and sensitivity to bias and random error in data sources?)
- 1436 V. Does it match local knowledge and concerns?
- 1437 VI. Can it be used to empower local stakeholders of watershed management through  
 1438 performance (outcome) based contracts?
- 1439 VII. Can it inform local risk management?  
 1440

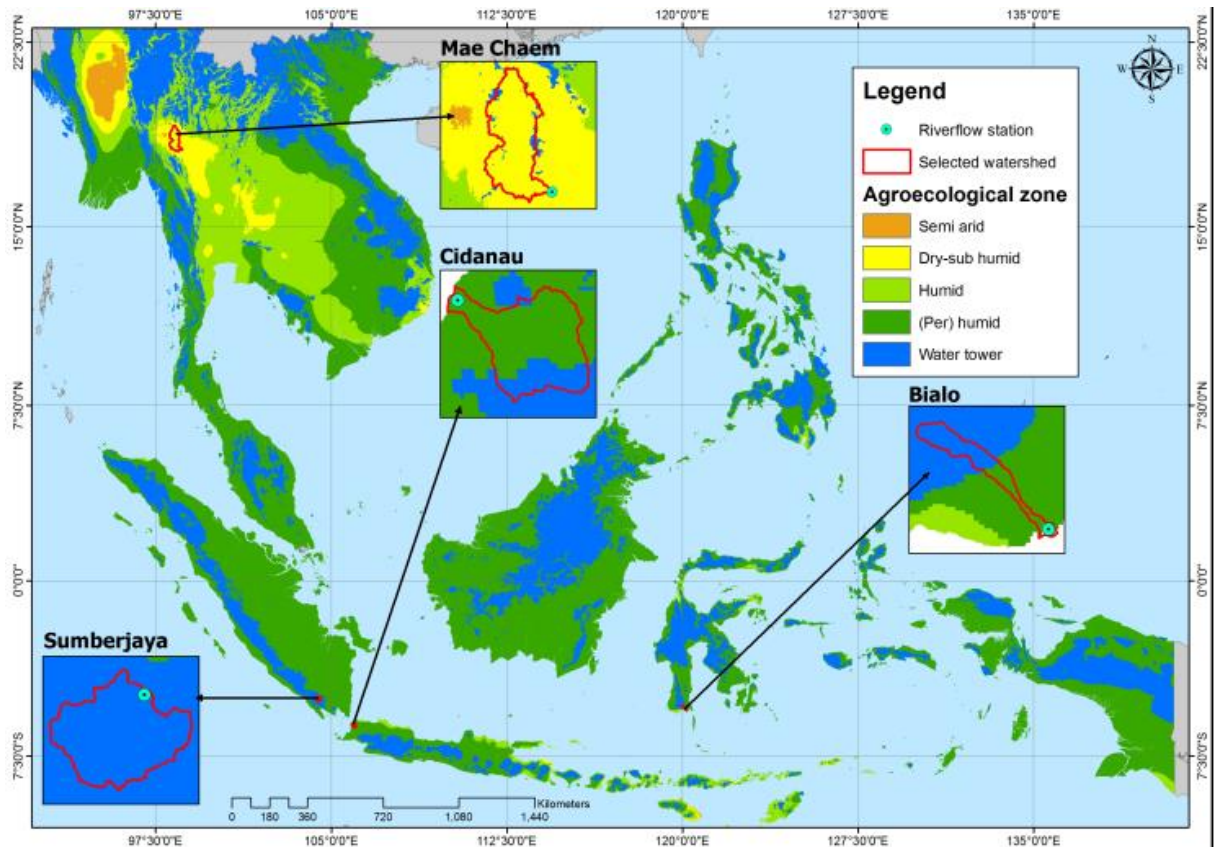
1441 Table 7. Data availability

	Bialo	Cidanau	Mae Chaem	Way Besai
Rainfall data	1989-2009, Source: BWS Sulawesi <sup>a</sup> and PUSAIR <sup>b</sup> ; Average rainfall data from the stations Moti, Bulobulo, Seka and Onto	1998-2008, source: BMKG <sup>c</sup>	1998-2002, source: WRD55, MTD22, RYP48, GMT13, WRD 52	1976-2007, Source: BMKG, PU <sup>d</sup> and PLN <sup>e</sup> (interpolation of 8 rainfall stations using Thiessen polygon)
River flow data	1993-2010, source; BWS Sulawesi and PUSAIR	2000-2009, source: KTI <sup>f</sup>	1954-2003, source: ICHARM <sup>g</sup>	1976-1998, source: PU and PUSAIR
Reference of detailed report	<a href="http://old.icraf.org/regions/southeast_asia/publications?do=view_pub_detail&amp;pub_no=PP0343-14">http://old.icraf.org/regions/southeast_asia/publications?do=view_pub_detail&amp;pub_no=PP0343-14</a>	<a href="http://worldagroforestry.org/regions/southeast_asia/publications?do=view_pub_detail&amp;pub_no=PO0292-13">http://worldagroforestry.org/regions/southeast_asia/publications?do=view_pub_detail&amp;pub_no=PO0292-13</a>	<a href="http://worldagroforestry.org/regions/southeast_asia/publications?do=view_pub_detail&amp;pub_no=MN0048-11">http://worldagroforestry.org/regions/southeast_asia/publications?do=view_pub_detail&amp;pub_no=MN0048-11</a>	<a href="http://worldagroforestry.org/regions/southeast_asia/publications?do=view_pub_detail&amp;pub_no=MN0048-11">http://worldagroforestry.org/regions/southeast_asia/publications?do=view_pub_detail&amp;pub_no=MN0048-11</a>

1442 Note:

1443 <sup>a</sup>BWS: Balai Wilayah Sungai (*Regional River Agency*)1444 <sup>b</sup>PUSAIR: Pusat Litbang Sumber Daya Air (*Centre for Research and Development on Water Resources*)1445 <sup>c</sup>BMKG: Badan Meteorologi Klimatologi dan Geofisika (*Agency on Meteorology, Climatology and Geophysics*)1447 <sup>d</sup>PU: Dinas Pekerjaan Unum (*Public Work Agency*)1448 <sup>e</sup>PLN: Perusahaan Listrik Negara (*National Electric Company*)1449 <sup>f</sup>KTI: Krakatau Tirta Industri, a private steel company1450 <sup>g</sup>ICHARM: The International Centre for Water Hazard and Risk Management

1451

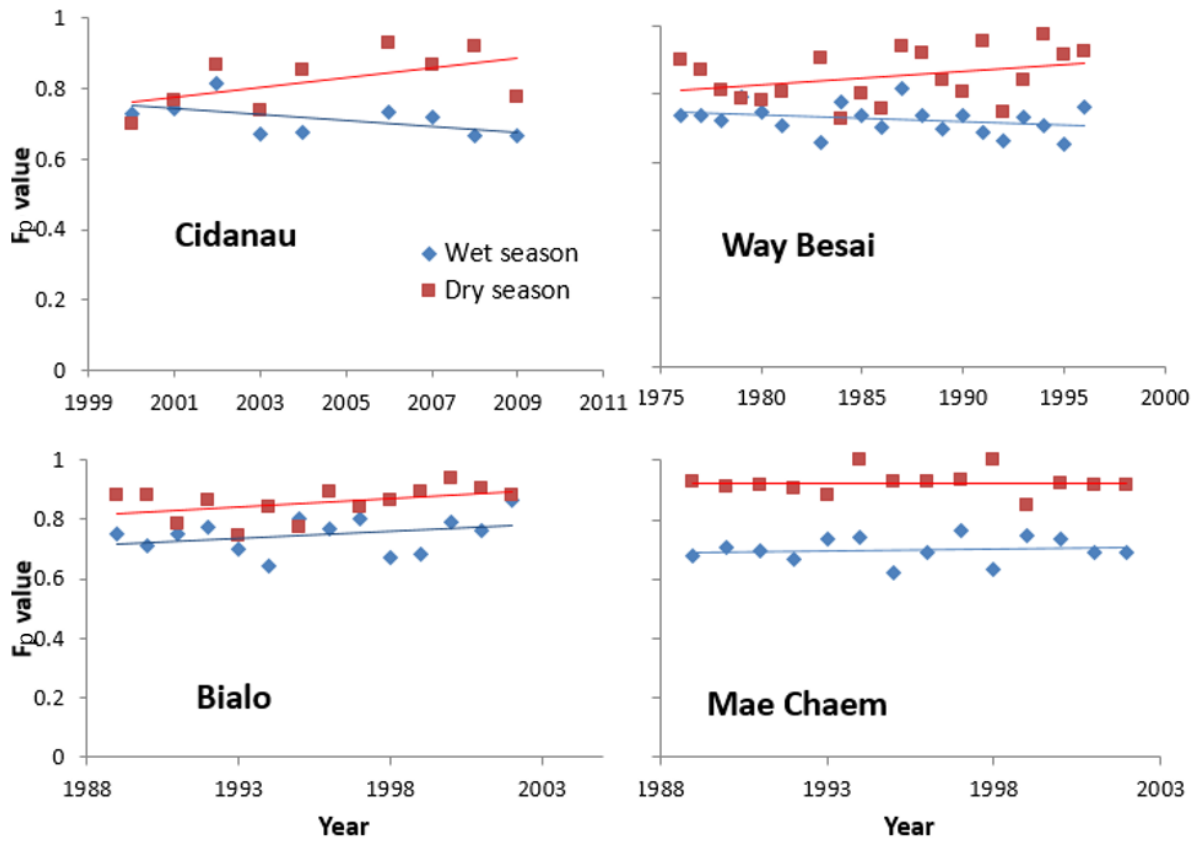


1452

1453 Figure 1. Location of the four watersheds in the agroecological zones of Southeast Asia (water  
1454 towers are defined on the basis of ability to generate river flow and being in the upper part of a  
1455 watershed)

1456

1457

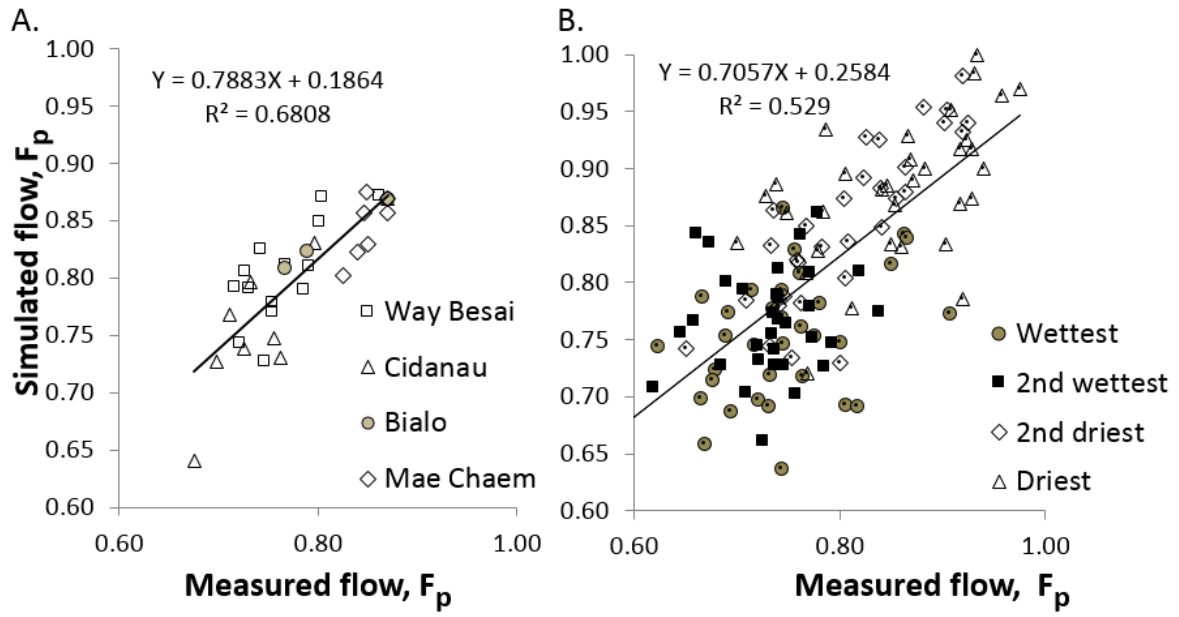


1458

1459 Figure 2. Flow persistence ( $F_p$ ) estimates derived from measurements in four Southeast Asian  
1460 watersheds, separately for the wettest and driest 3-month periods of the year

1461

1462

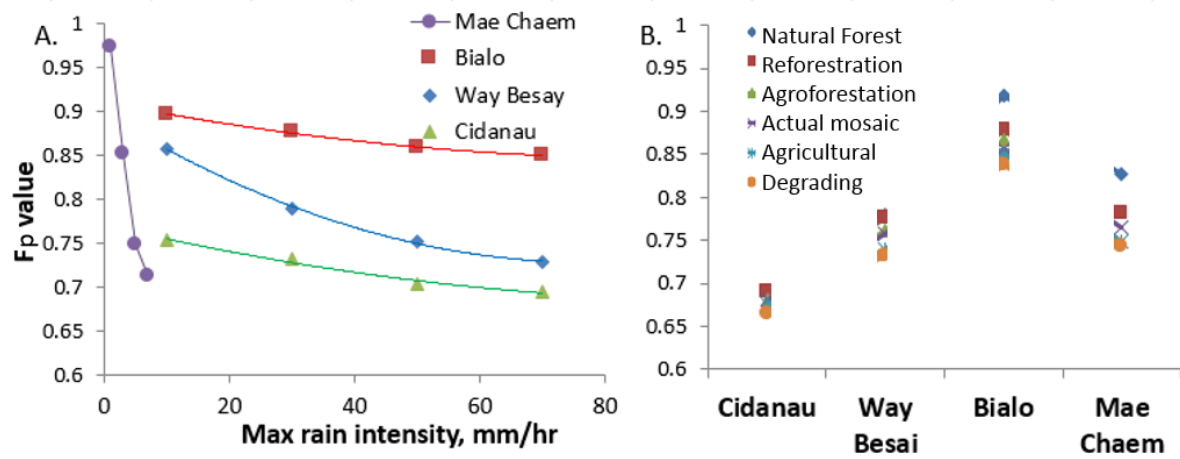


1463

1464 Figure 3. Inter- (A) and intra- (B) annual variation in the  $F_p$  parameter derived from empirical versus  
 1465 modelled flow: for the four test sites on annual basis (A) or three-monthly basis (B)

1466

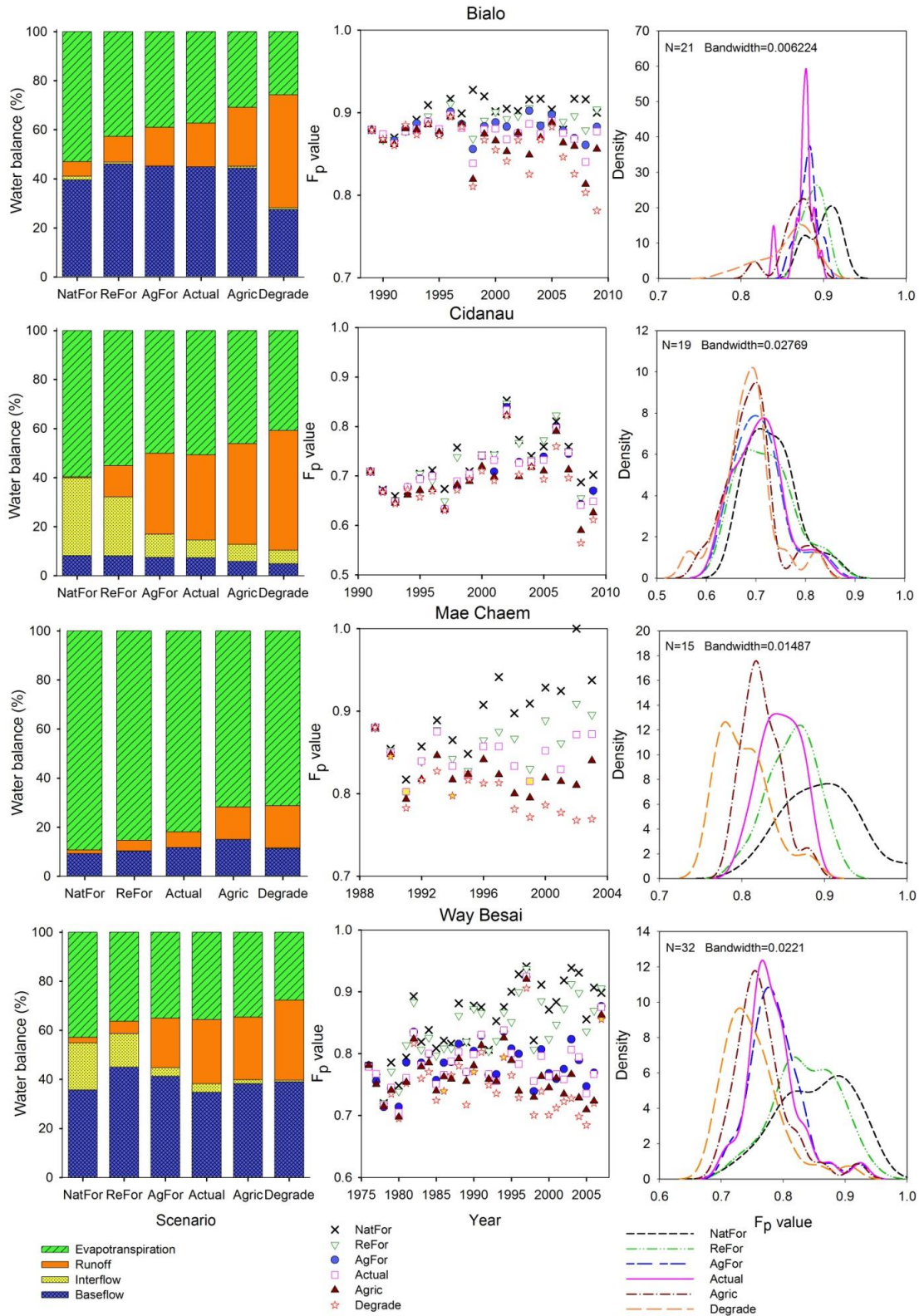
1467



1468

1469 Figure 4 Effects on flow persistence of changes in A) the mean rainfall intensity and B) the land use  
 1470 change scenarios of Table 4 across the four watersheds

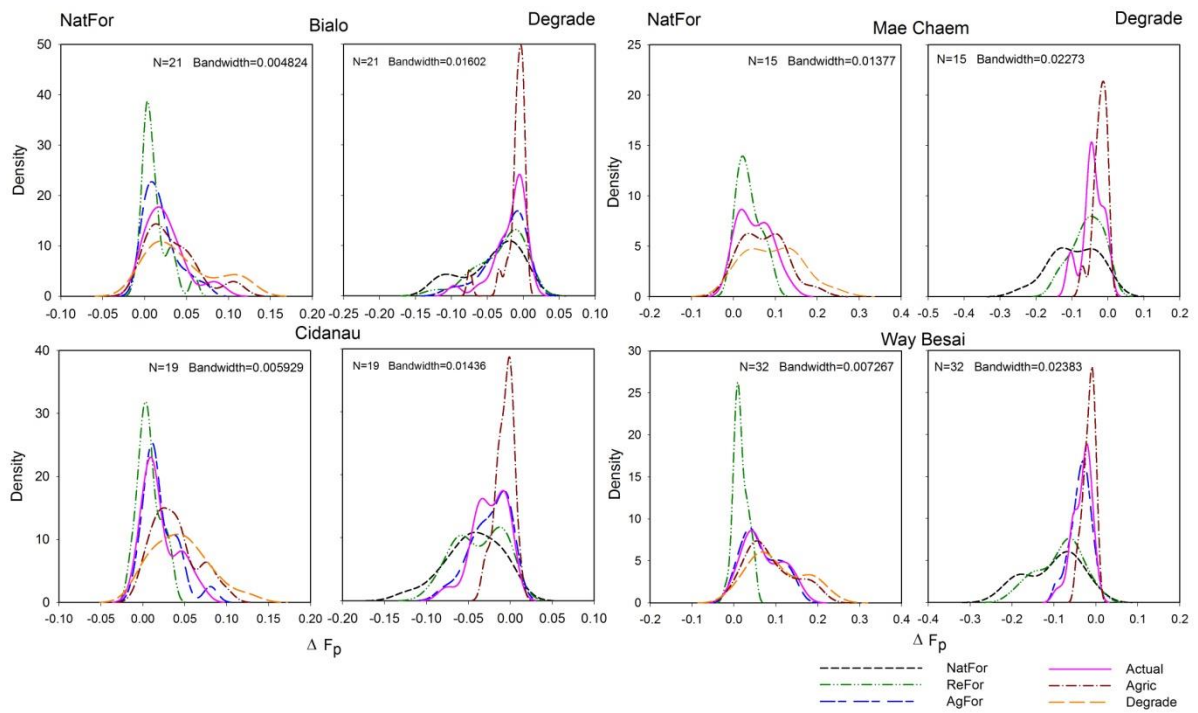
1471



1472

1473 Figure 5. Effects of land cover change scenarios (Table 4) on the flow persistence value in four  
 1474 watersheds, modelled in GenRiver over a 20-year time-period, based on actual rainfall records;  
 1475 the left side panels show average water balance for each land cover scenario, the middle panels  
 1476 the Fp values per year and land use, the right-side panels the derived frequency distributions  
 1477 (best fitting Weibull distribution)

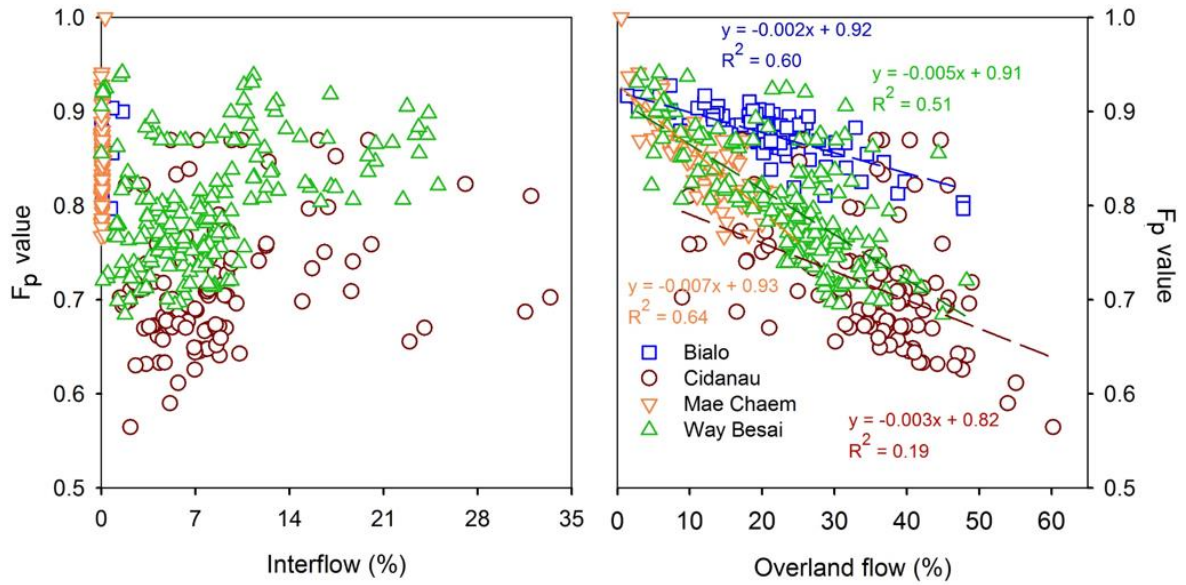
1478



1479

1480 Figure 6. Frequency distribution of expected difference in  $F_p$  in 'paired plot' comparisons where land  
1481 cover is the only variable; left panels: all scenarios compared to 'Reforestation', right panel: all  
1482 scenarios compared to degradation; graphs are based on a kernel density estimation (smoothing)  
1483 approach

1484

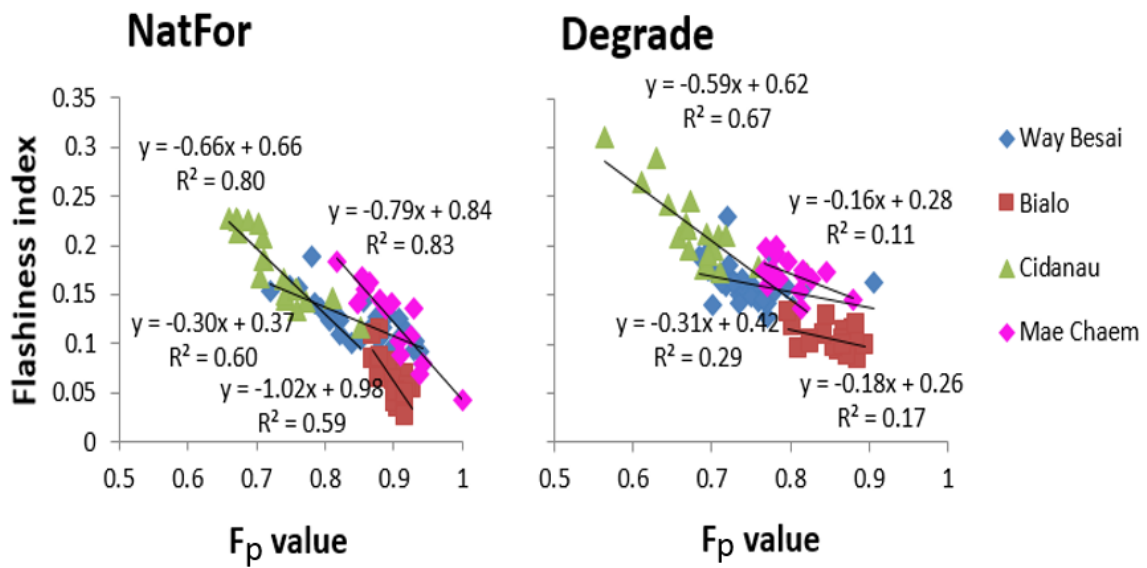


1485

1486 Figure 7. Correlations of  $F_p$  with fractions of rainfall that take overland flow and interflow pathways

1487 through the watershed, across all years and land use scenarios of Figure App2

1488



1489

1490 Figure 8. Relationship between  $F_p$  value and R-B Flashiness index across years in four Southeast Asian

1491 watersheds under a 'natural forest' and 'degradation' scenario, simulated with the GenRiver model

1492 Appendix 1. GenRiver model for effects of land cover on river flow

1493 The Generic River flow (GenRiver) model (van Noordwijk et al., 2011) is a simple hydrological model  
 1494 that simulates river flow based on water balance concept with a daily time step and a flexible spatial  
 1495 subdivision of a watershed that influences the routing of water. The core of the GenRiver model is a  
 1496 “patch” level representation of a daily water balance, driven by local rainfall and modified by the  
 1497 land cover and land cover change and soil properties. The model starts accounting of rainfall or  
 1498 /precipitation (P) and traces the subsequent flows and storage in the landscape that can lead to  
 1499 either evapotranspiration (E), river flow (Q) or change in storage ( $\Delta S$ ) (Figure App1):

1500  $P = Q + E + \Delta S$  [1]

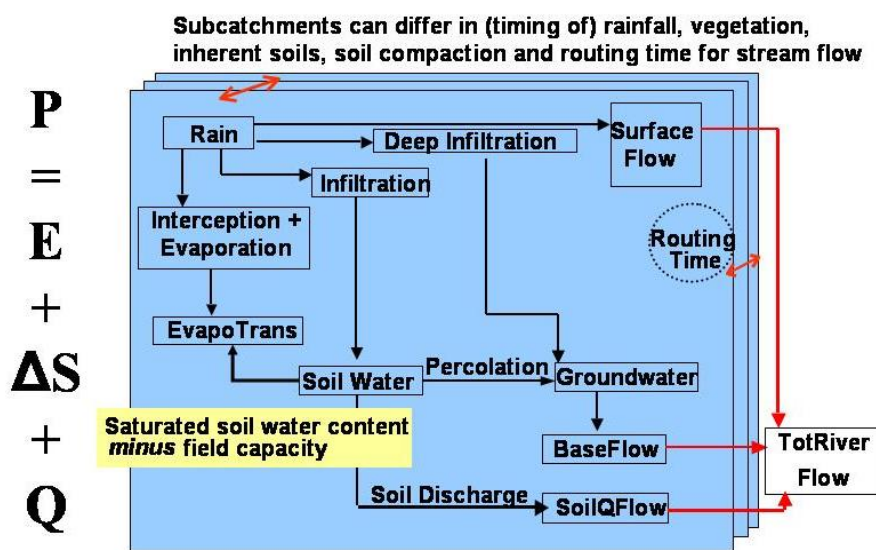


Figure App1. Overview of the GenRiver model

1501

1502 The model may use measured rainfall data, or use a rainfall generator that involves Markov chain  
 1503 temporal autocorrelation (rain persistence). The model can represent spatially explicit rainfall, with  
 1504 stochastic rainfall intensity (parameters RainIntensMean, RainIntensCoefVar in Table 2) and partial  
 1505 spatial correlation of daily rainfall between subcatchments. Canopy interception leads to direct  
 1506 evaporation of an amount of water controlled by the thickness of waterfilm on the leaf area that  
 1507 depends on the land cover, and a delay of water reaching the soil surface (parameter  
 1508 RainMaxIntDripDur in Table 2). The effect of evaporation of intercepted water on other components  
 1509 of evapotranspiration is controlled by the InterceptEffectontrans parameter that in practice may  
 1510 depend on the time of day rainfall occurs and local climatic conditions such as windspeed)

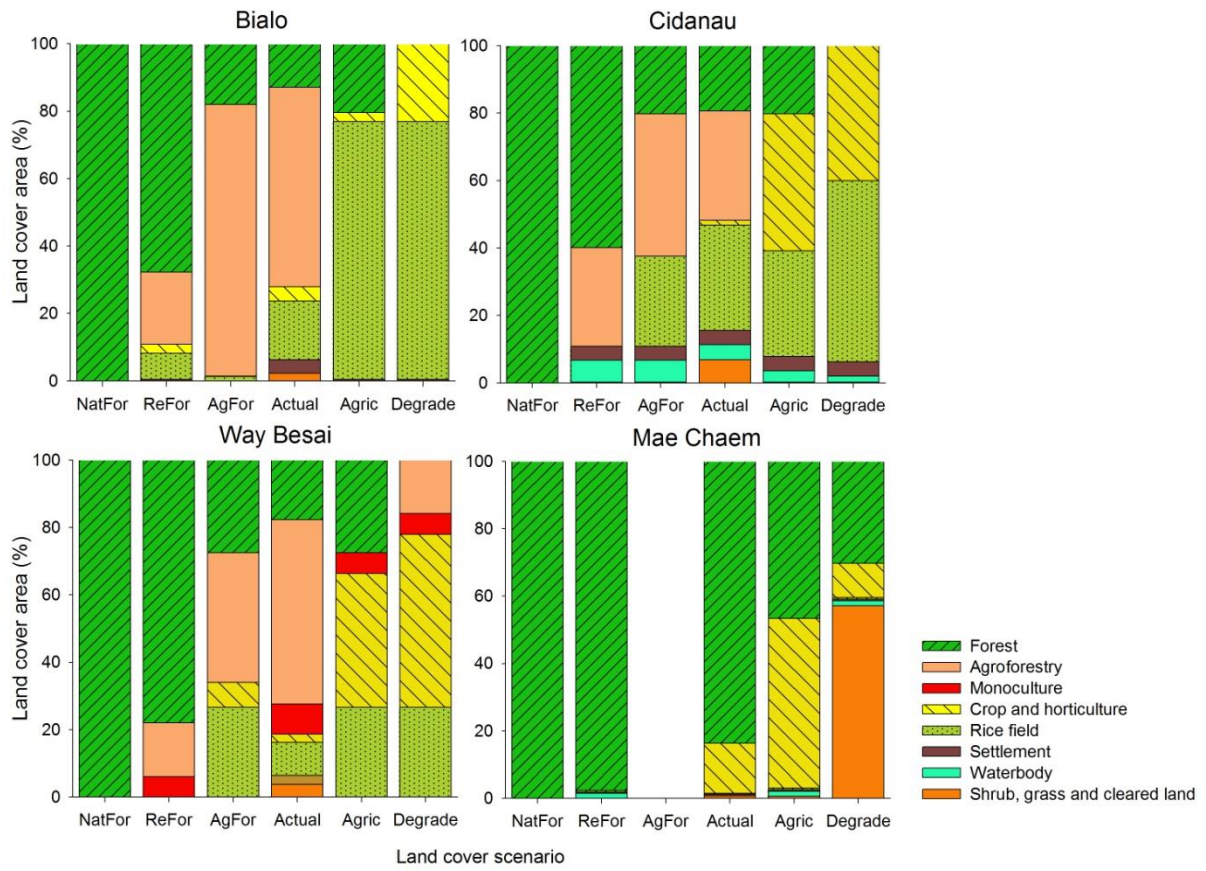
1511 At patch level, vegetation influences interception, retention for subsequent evaporation and delayed  
 1512 transfer to the soil surface, as well as the seasonal demand for water. Vegetation (land cover) also  
 1513 influences soil porosity and infiltration, modifying the inherent soil properties. Groundwater pool  
 1514 dynamics are represented at subcatchment rather than patch level, integrating over the landcover  
 1515 fractions within a subcatchment. The output of the model is river flow which is aggregated from  
 1516 three types of stream flow: surface flow on the day of the rainfall event; interflow on the next day;  
 1517 and base flow gradually declining over a period of time. The multiple subcatchments that make up

1518 the catchment as a whole can differ in basic soil properties, land cover fractions that affect  
1519 interception, soil structure (infiltration rate) and seasonal pattern of water use by the vegetation.  
1520 The subcatchment will also typically differ in “routing time” or in the time it takes the streams and  
1521 river to reach any specified observation point (with default focus on the outflow from the  
1522 catchment). The model itself (currently implemented in Stella plus Excel), a manual and application  
1523 case studies are freely available ([http://www.worldagroforestry.org/output/genriver-generic-river-](http://www.worldagroforestry.org/output/genriver-generic-river-model-river-flow)  
1524 [model-river-flow](http://www.worldagroforestry.org/output/genriver-generic-river-model-river-flow) ;van Noordwijk et al., 2011).

1525

1526 Appendix 2. Watershed-specific consequences of the land use change scenarios

1527 The generically defined land use change scenarios (Table 4) led to different land cover proportions,  
1528 depending on the default land cover data for each watershed, as shown in Figure App2.



1529

1530 Figure App2. Land use distribution of the various land use scenarios explored for the four

1531 watersheds (see Table 4)

1532

```

1533 Appendix 3. Example of a macro in R to estimate number of observation required using bootstrap
1534 approach.
1535
1536 #The bootstrap procedure is to calculate the minimum sample size (number of observation) required
1537 #for a significant land use effect on Fp
1538 #bialo1 is a dataset contains delta Fp values for two different from Bialo watershed
1539
1540 #read data
1541 bialo1 <- read.table("bialo1.csv", header=TRUE, sep=",")
1542
1543 #name each parameter
1544 BL1 <- bialo1$ReFor
1545 BL5 <- bialo1$Degrade
1546
1547 N = 1000 #number replication
1548
1549 n <- c(5:50) #the various sample size
1550
1551 J <- 46 #the number of sample size being tested (~ number of actual year observed in the dataset)
1552
1553 P15= matrix(ncol=J, nrow=R) #variable for storing p-value
1554 P15Q3 <- numeric(J) #for storing p-Value at 97.5 quantile
1555
1556 for (j in 1:J) #estimating for different n
1557
1558 #bootstrap sampling
1559 {
1560 for (i in 1:N)
1561 {
1562 #sampling data
1563 S1=sample(BL1, n[j], replace = T)
1564 S5=sample(BL5, n[j], replace = T)
1565
1566 #Kolmogorov-Smirnov test for equal distribution and get the p-Value
1567 KS15 <- ks.test(S1, S5, alt = c("two.sided"), exact = F) P15[i,j] <- KS15$p.value
1568 }
1569
1570 #Confidence interval of CI
1571 P15Q3[j] <- quantile(P15[,j], 0.975)
1572
1573 }
1574
1575 #saving P value data and CI
1576

```

```
1577 write.table(P15, file = "pValue15.txt") write.table(P15Q3, file = "P15Q3.txt")v
1578 /
```